Performance of Lagrangian Finite Volume Approaches for Linear and Nonlinear Solid Mechanics Analyses

Philip Cardiff

26th to 30th June 2016

11th OpenFOAM Workshop
Vila Flor Cultural Centre
Guimarães, Portugal

Performance of Lagrangian Finite Volume Approaches for Linear and Nonlinear Solid Mechanics Analyses

Philip Cardiff

Željko Tukovic
Michael Clancy
Hrvoje Jasak
Peter De Jaeger
Alojz Ivanković

School of Mechanical and Materials Engineering
University College Dublin

better together

Irish Centre for Composites Research

Background & Motivation

Background

Historically

Computational Solid Mechanics **=** **Finite Element Method**

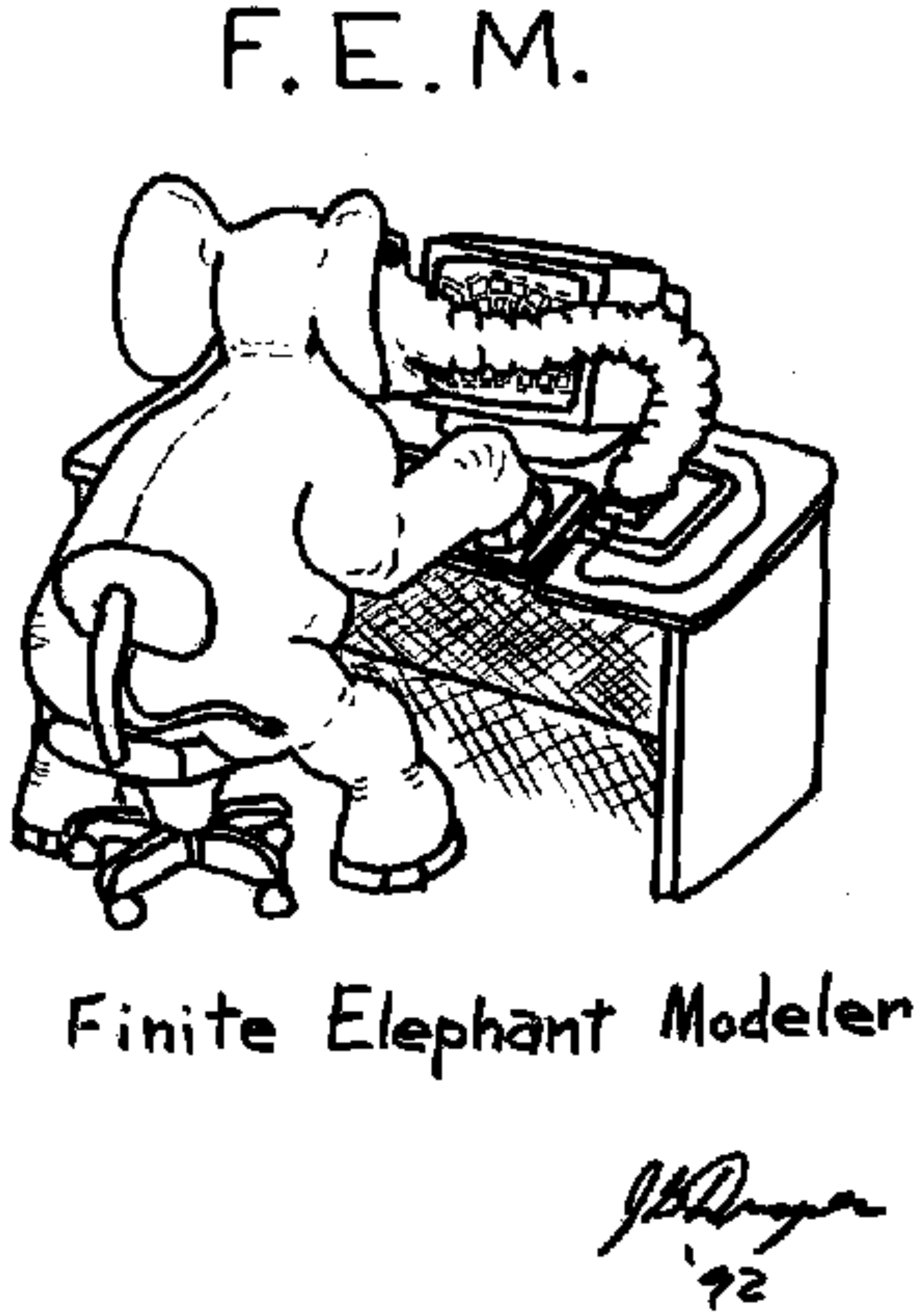

… but alternative approaches, such as the **Finite Volume Method**, are gaining traction …

Motivation

There are a number of motivations for pursuing FV-based solid mechanics:

- complex nonlinear multi-physics applications
- Fluid-Solid Interaction within the same numerical framework
- the relative success of OpenFOAM for CFD has led to a desire for equivalent solid mechanics procedures within the library
- academic interest …

Let's look at some of the latest FV solid mechanics in OpenFOAM.

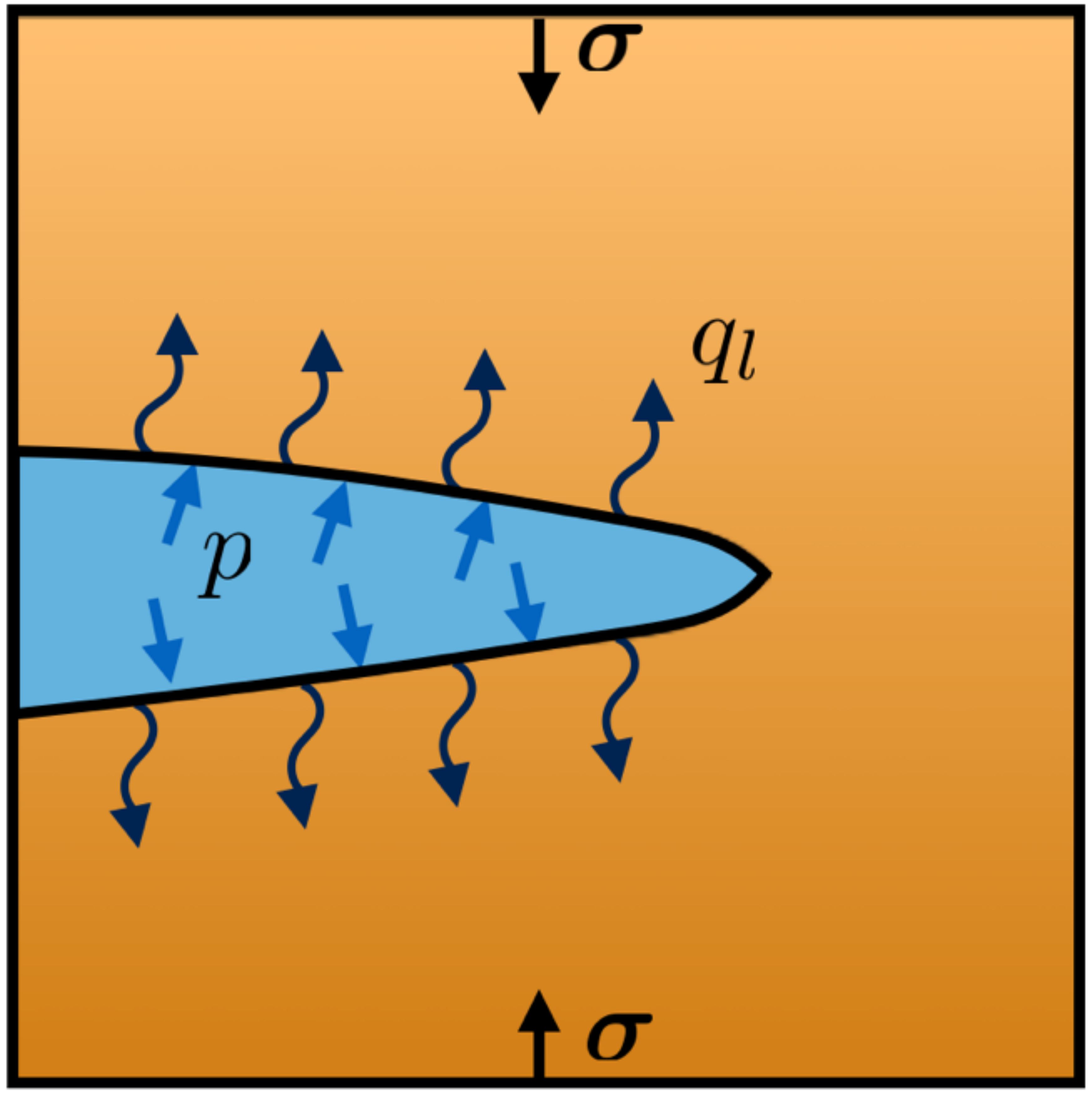

$$\oint_{\Gamma} \boldsymbol{n} \cdot \boldsymbol{D} \, d\Gamma - \int_{\Omega} Q \, d\Omega = 0$$

$$\rho \frac{\partial^2 u}{\partial t^2} = \nabla \cdot \sigma$$

$$\rho C \frac{\partial T}{\partial t} = k \nabla^2 T$$

Finite Volume Method for Solid Mechanics

Mathematical Model

Conservation of Linear Momentum

$$\underbrace{\frac{D}{Dt}\int_{\Omega} \rho \boldsymbol{v} \, \mathrm{d}\Omega}_{\text{change in momentum}} = \underbrace{\int_{\Gamma} \boldsymbol{n} \cdot \boldsymbol{\sigma} \, \mathrm{d}\Gamma}_{\text{sum of surface forces}} + \underbrace{\int_{\Omega} \rho \boldsymbol{f}_b \, \mathrm{d}\Omega}_{\text{sum of body forces}}$$

Let us consider two contrasting constitutive relations:

Hooke's law (small strains/rotations, linear):

$$\boldsymbol{\sigma} = 2\mu\boldsymbol{\epsilon} + \lambda\,\mathrm{tr}(\boldsymbol{\epsilon})\mathbf{I}$$

Neo-Hookean hyperelastoplastic law (large strains/rotations nonlinear):

$$\boldsymbol{\sigma} = J\left[\mu\,\mathrm{dev}(\bar{\boldsymbol{b}}^e) - \frac{\kappa}{2}\left(J^2 - 1\right)\mathbf{I}\right]$$

Calculated from Mises-Huber-Levy J_2 plasticity

Inserting the constitutive relation into the governing equation gives the mathematical model:

Hookean linear elastic solid:

$$\rho \frac{\partial^2 \boldsymbol{u}}{\partial t^2} = \boldsymbol{\nabla} \cdot (\mu \boldsymbol{\nabla} \boldsymbol{u}) + \boldsymbol{\nabla} \cdot \left(\mu (\boldsymbol{\nabla} \boldsymbol{u})^T\right) + \boldsymbol{\nabla} \cdot (\lambda \mathrm{tr}(\boldsymbol{\nabla} \boldsymbol{u}) \mathbf{I}) + \rho \boldsymbol{f}_b$$

Neo-Hookean nonlinear hyperelastoplastic solid (updated Lagrangian formulation):

$$\rho \frac{\partial^2 \boldsymbol{u}}{\partial t^2} = \boldsymbol{\nabla} \cdot \left(j \boldsymbol{\sigma} \cdot \boldsymbol{f}^{-T} \right) + \rho \boldsymbol{f}_b$$

Solution algorithm: **block-coupled**

Hookean linear elastic solid:

$$\rho \frac{\partial^2 \boldsymbol{u}}{\partial t^2} = \boldsymbol{\nabla} \cdot (\mu \boldsymbol{\nabla} \boldsymbol{u}) + \boldsymbol{\nabla} \cdot \left(\mu (\boldsymbol{\nabla} \boldsymbol{u})^T\right) + \boldsymbol{\nabla} \cdot (\lambda \mathrm{tr}(\boldsymbol{\nabla} \boldsymbol{u}) \mathbf{I}) + \rho \boldsymbol{f}_b$$

`fvm::laplacian` `fvm::laplacianTranspose` `fvm::laplacianTrace`

… not implemented in OpenFOAM …

… we need to do it ourselves.

Solution algorithm: **segregated**

Neo-Hookean nonlinear hyperelastoplastic solid:

$$\rho \frac{\partial^2 \boldsymbol{u}}{\partial t^2} = \overbrace{K_{\text{imp}} \boldsymbol{\nabla}^2 (\Delta \boldsymbol{u})}^{\text{implicit}} + \overbrace{\boldsymbol{\nabla} \cdot \left(j \boldsymbol{\sigma} \cdot \boldsymbol{f}^{-T} \right) - K_{\text{imp}} \boldsymbol{\nabla}^2 (\Delta \boldsymbol{u})}^{\text{explicit}}$$

`fvm::laplacian` (implicit term) → `fvc::div` (explicit term)

Block-Coupled Challenges:
Equation
Discretisation

Normal Gradient Discretisation

Normal derivatives approximated using central differencing

$$\oint_\Gamma (2\mu + \lambda)\nabla_n u_n \, \mathrm{d}|\Gamma| \approx \sum_f (2\mu_f + \lambda_f)|\boldsymbol{\Delta}_f|(\boldsymbol{n}_f \boldsymbol{n}_f) \cdot \left(\frac{\boldsymbol{u}^N - \boldsymbol{u}^P}{|\boldsymbol{d}_f|} \right) |\boldsymbol{\Gamma}_f|$$

$$+ \sum_f (2\mu_f + \lambda_f)(\boldsymbol{n}_f \boldsymbol{n}_f) \cdot \left[\boldsymbol{k}_f \cdot (\nabla_t \boldsymbol{u})_f \right] |\boldsymbol{\Gamma}_f|$$

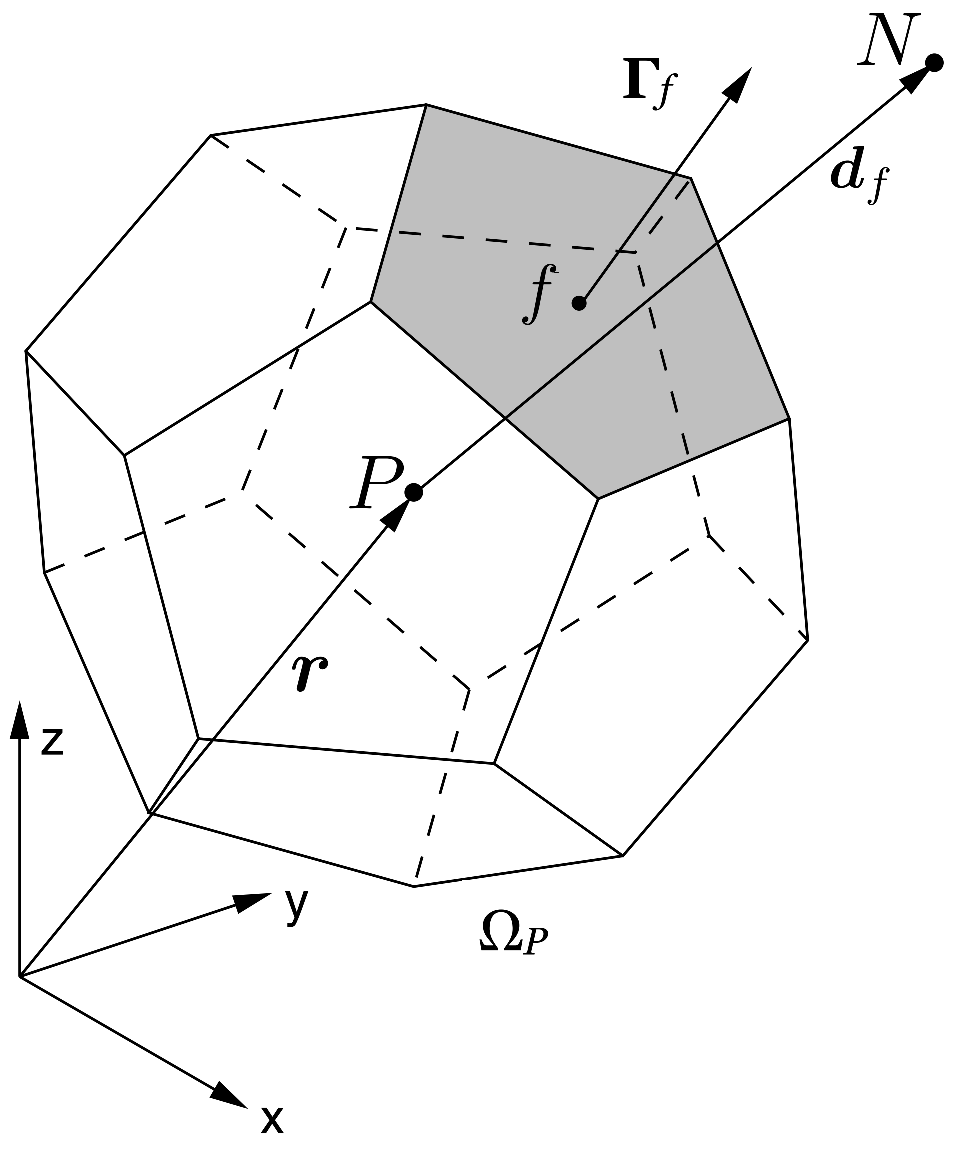

non-orthogonal correction implicitly discretised (see next slide); even gradient term is treated implicitly!

Tangential Gradient Discretisation

Tangential derivatives approximated using Finite Area Method

$$(\nabla_t u_n)_f = \frac{1}{|\boldsymbol{\Gamma}_f|} \sum_e \boldsymbol{m}_e (\boldsymbol{u}_n)_e \, L_e$$

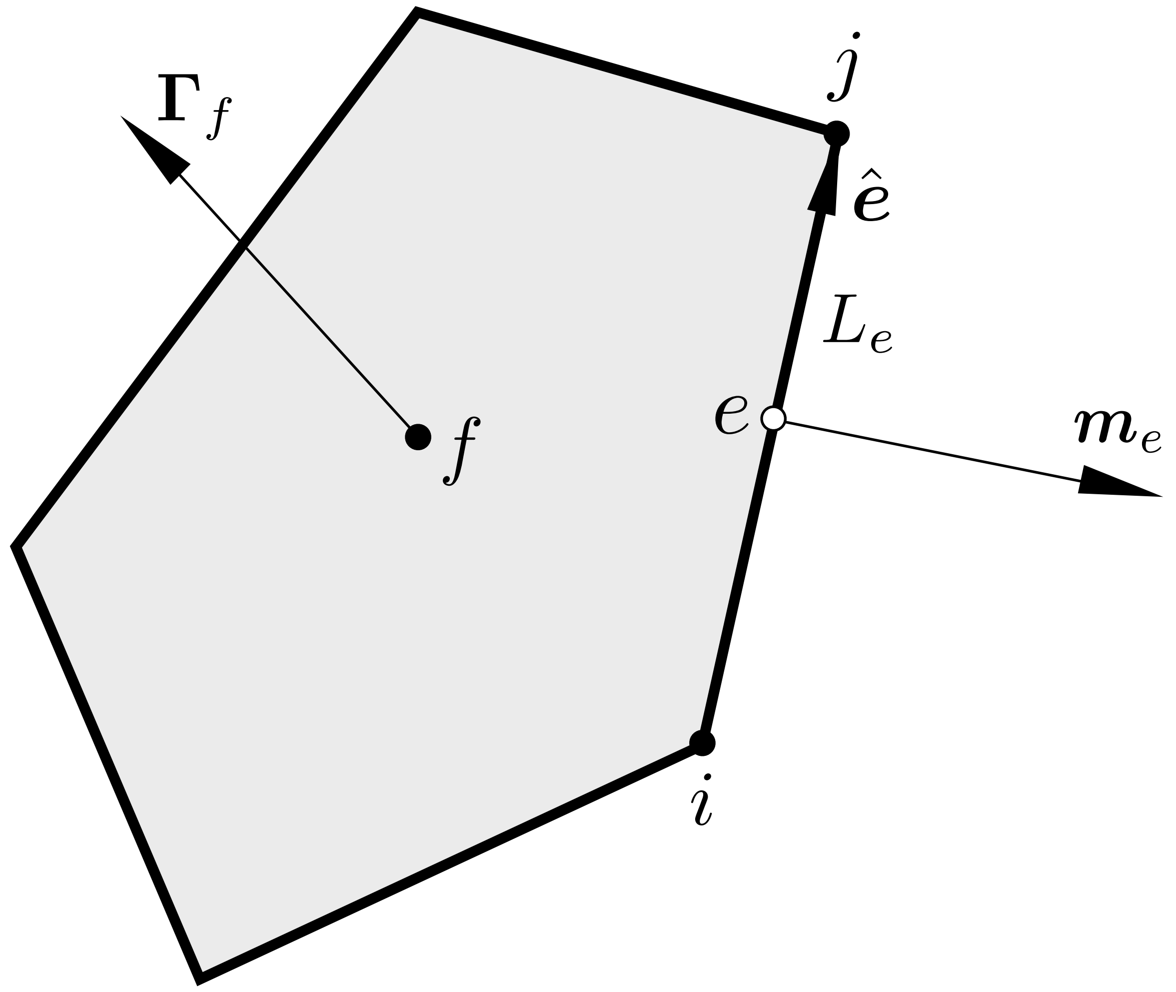

$$\oint_\Gamma \mu \nabla_t u_n \, \mathrm{d}\Gamma \approx \sum_f \sum_e \sum_{pc} \boxed{\frac{1}{2} \mu_f \omega_{pc} L_e (\boldsymbol{m}_e \boldsymbol{n}_f)} \cdot \boldsymbol{u}^{pc}$$

our coefficients!

$$\oint_\Gamma \lambda \, \boldsymbol{n} \, \mathrm{tr}\left(\nabla_t \boldsymbol{u}_t\right) \, \mathrm{d}\Gamma \approx \sum_f \sum_e \sum_{pc} \boxed{\frac{1}{2} \lambda_f \omega_{pc} L_e (\boldsymbol{m}_e \boldsymbol{n}_f)^T} \cdot \boldsymbol{u}^{pc}$$

```
solve
(
    magic::div(sigma)
)
```

Block-Coupled Challenges:
Implementation

Sparse Matrices in OpenFOAM

OpenFOAM fvMesh uses a sparse matrix addressing based on the mesh internal faces: only near-neighbours may be included implicitly in the matrix.

BUT, we require cell-point-cell neighbours to be included implicitly.

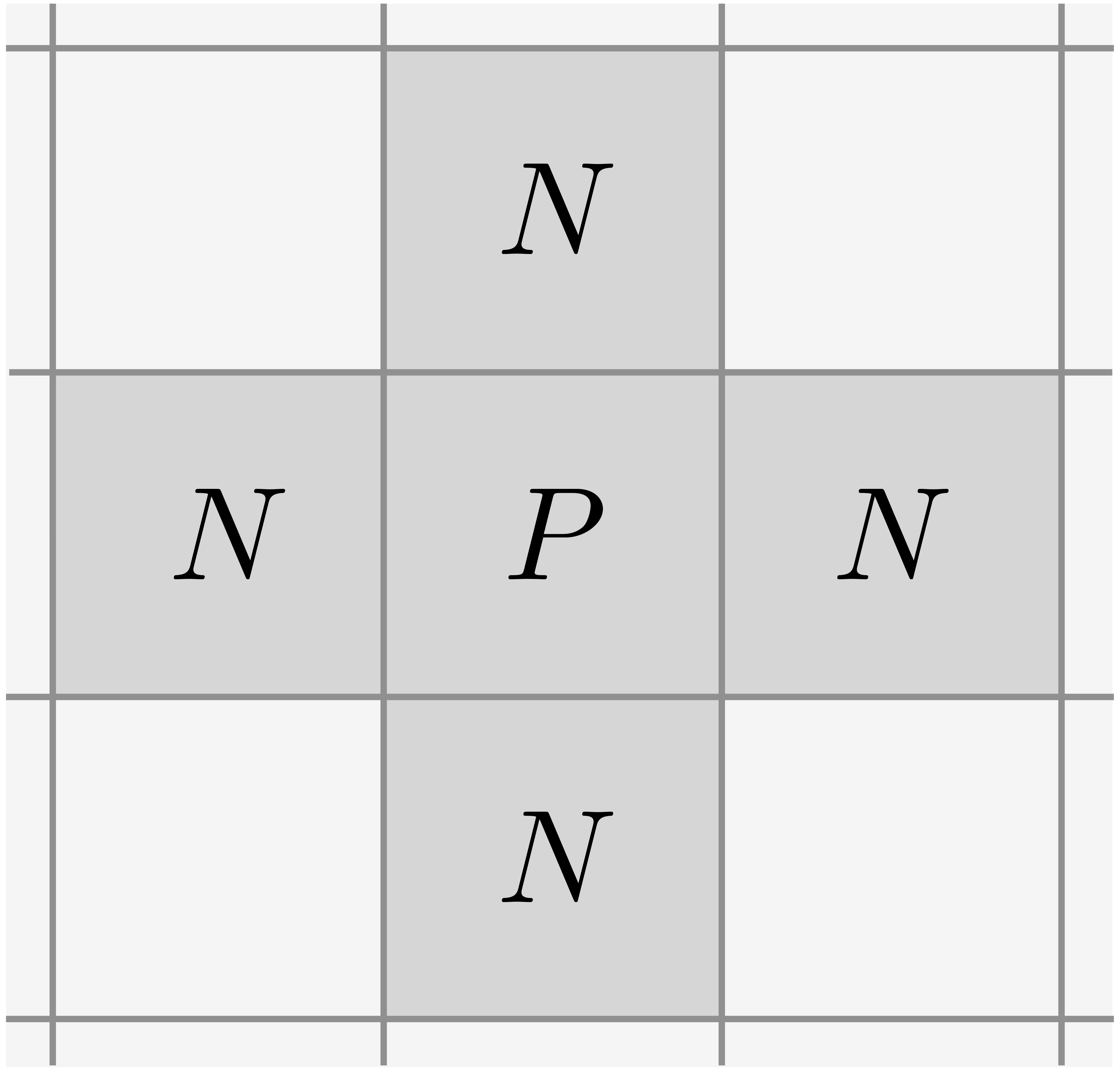

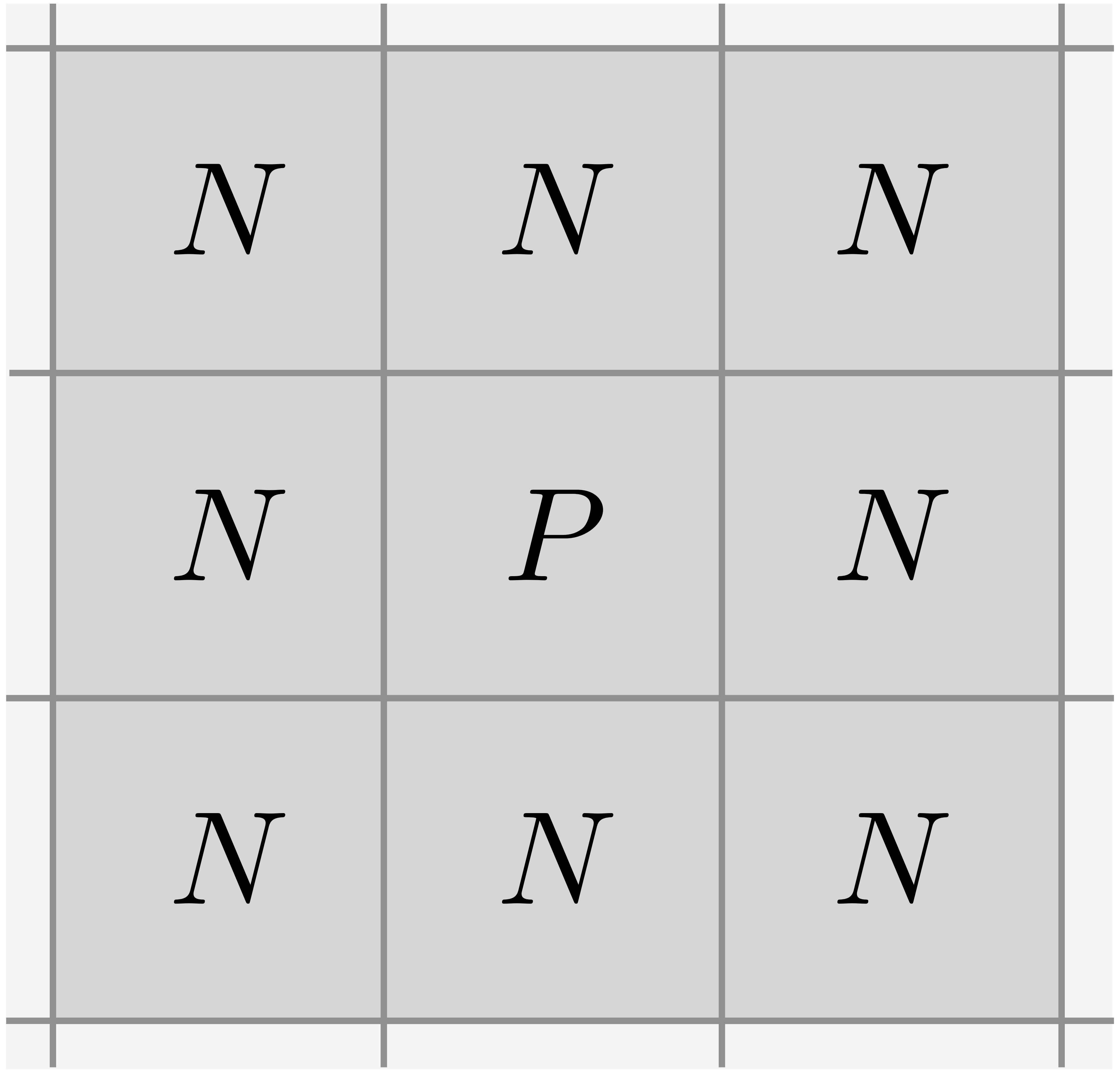

New Sparse Matrix Addressing Required

Let us refer to the matrix connections as implicit bonds

- Standard addressing allows implicit bonds with face neighbours
- New addressing must allow implicit bonds with point neighbours

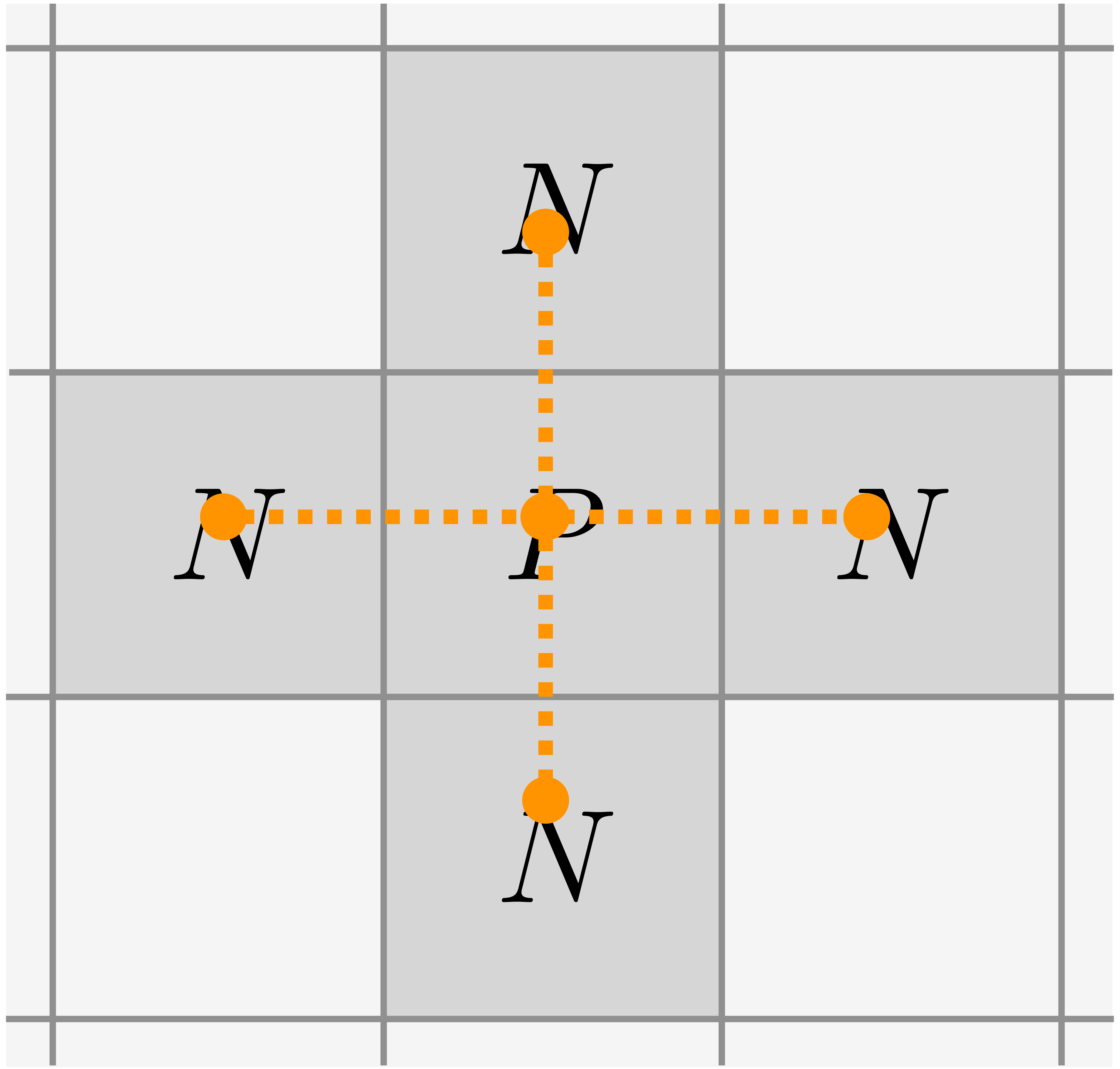

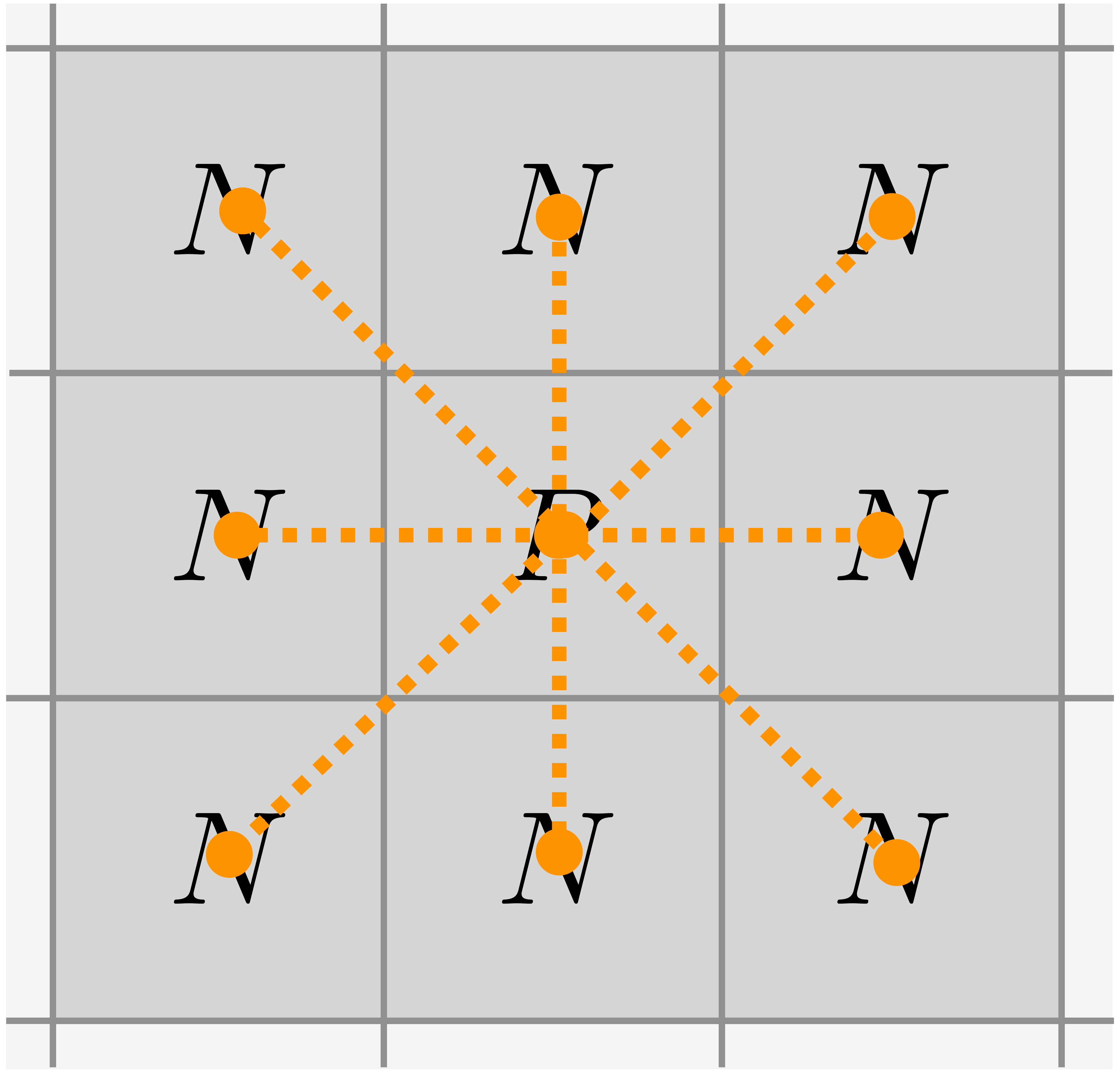

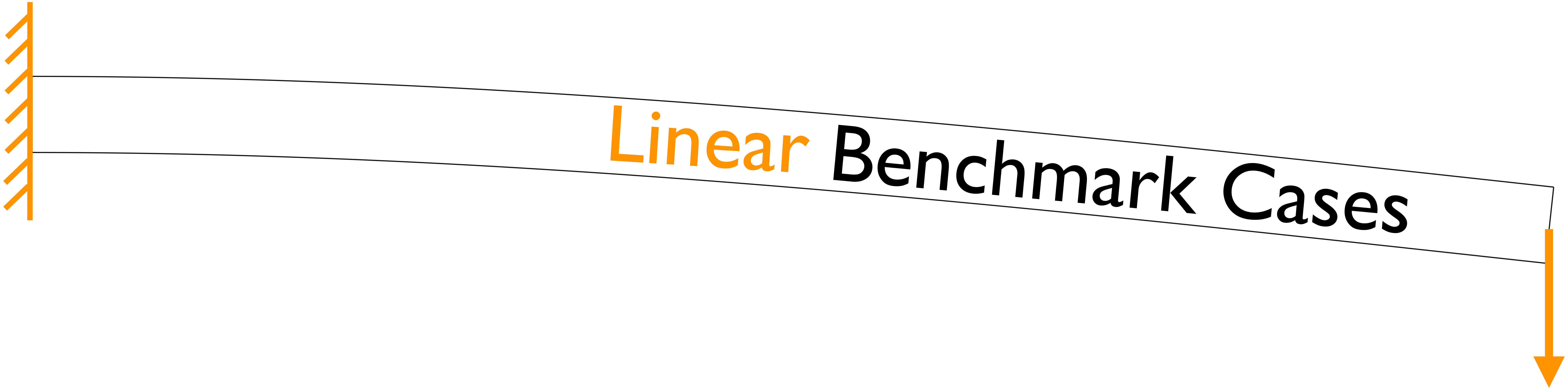
Linear Benchmark Cases

Out-of-Plane Bending of an Elliptic Plate

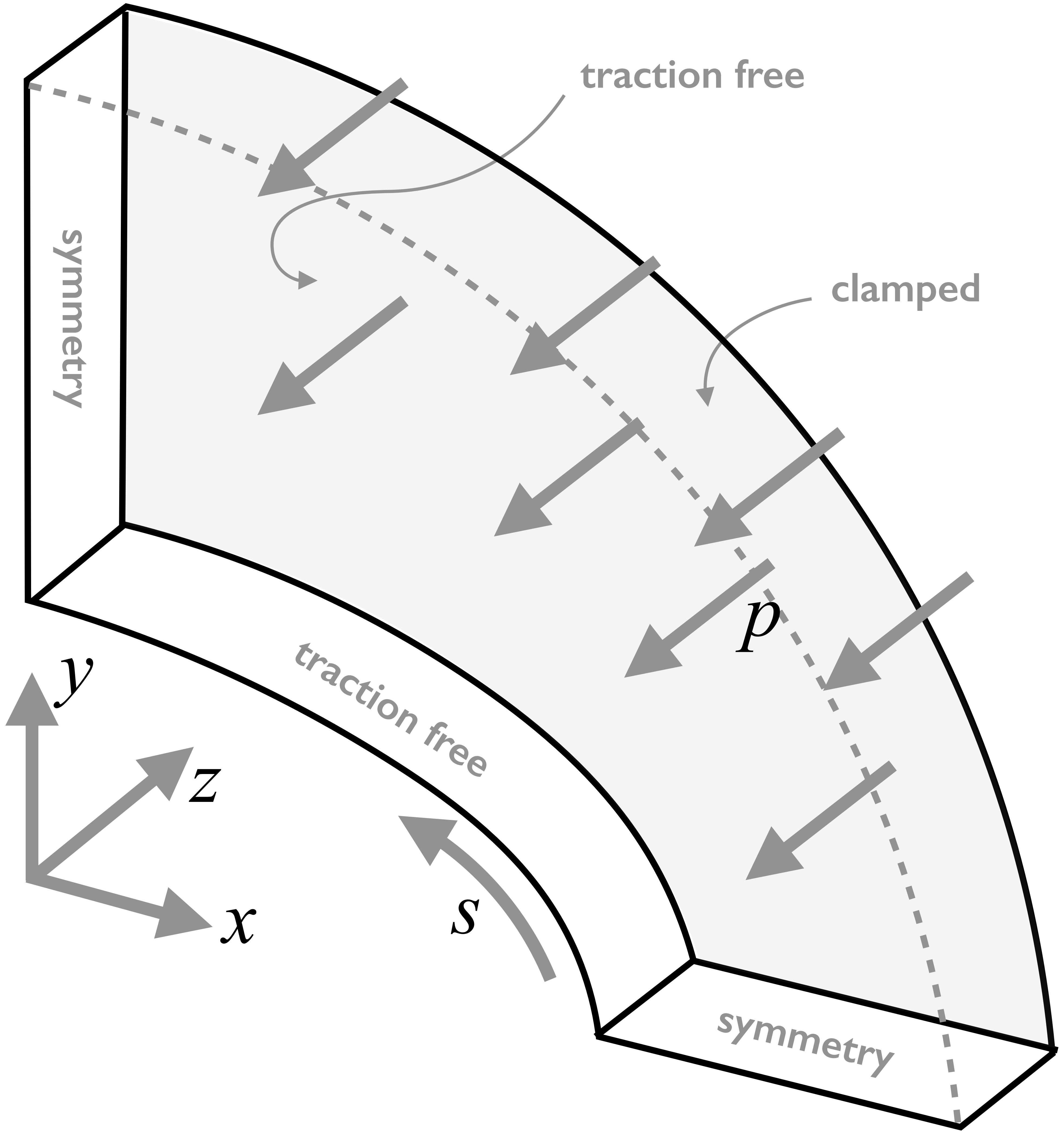

$$\left(\frac{x}{2}\right)^2 + \left(\frac{y}{1}\right)^2 = 1 \quad \text{inner ellipse}$$

$$\left(\frac{x}{3.25}\right)^2 + \left(\frac{y}{2.75}\right)^2 = 1 \quad \text{outer ellipse}$$

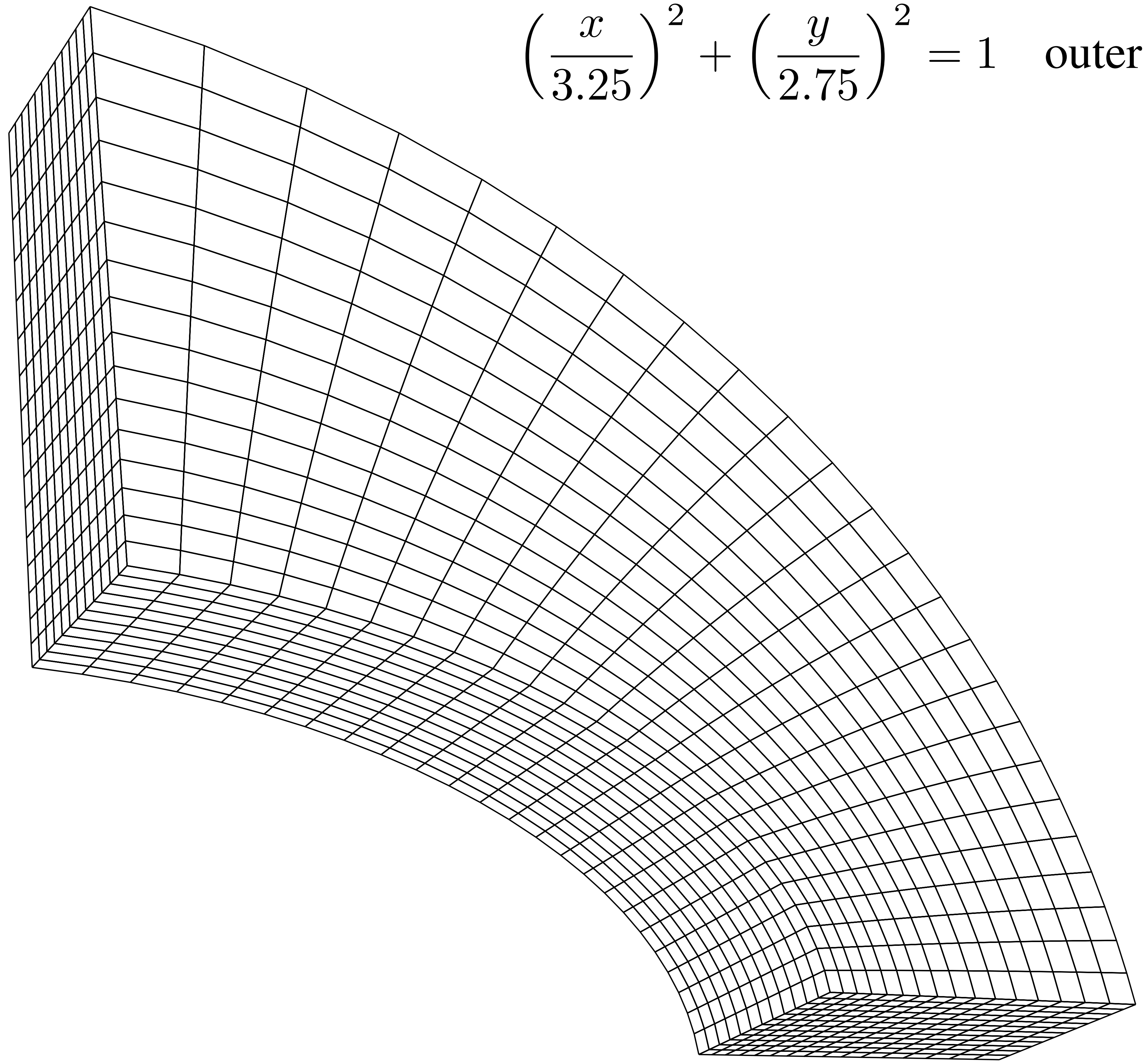

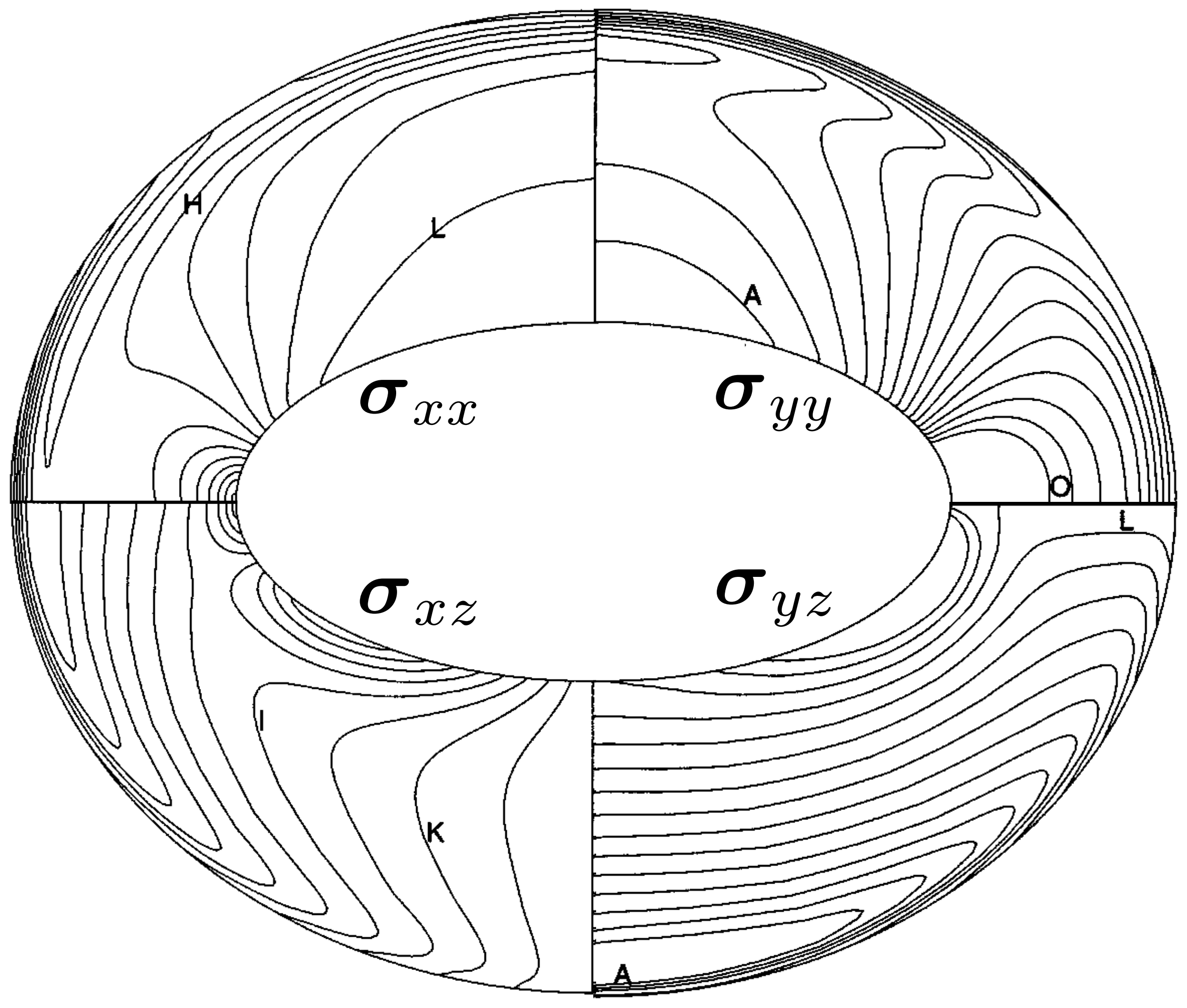

(a) Demirdžić et al. [3] Reference Solution

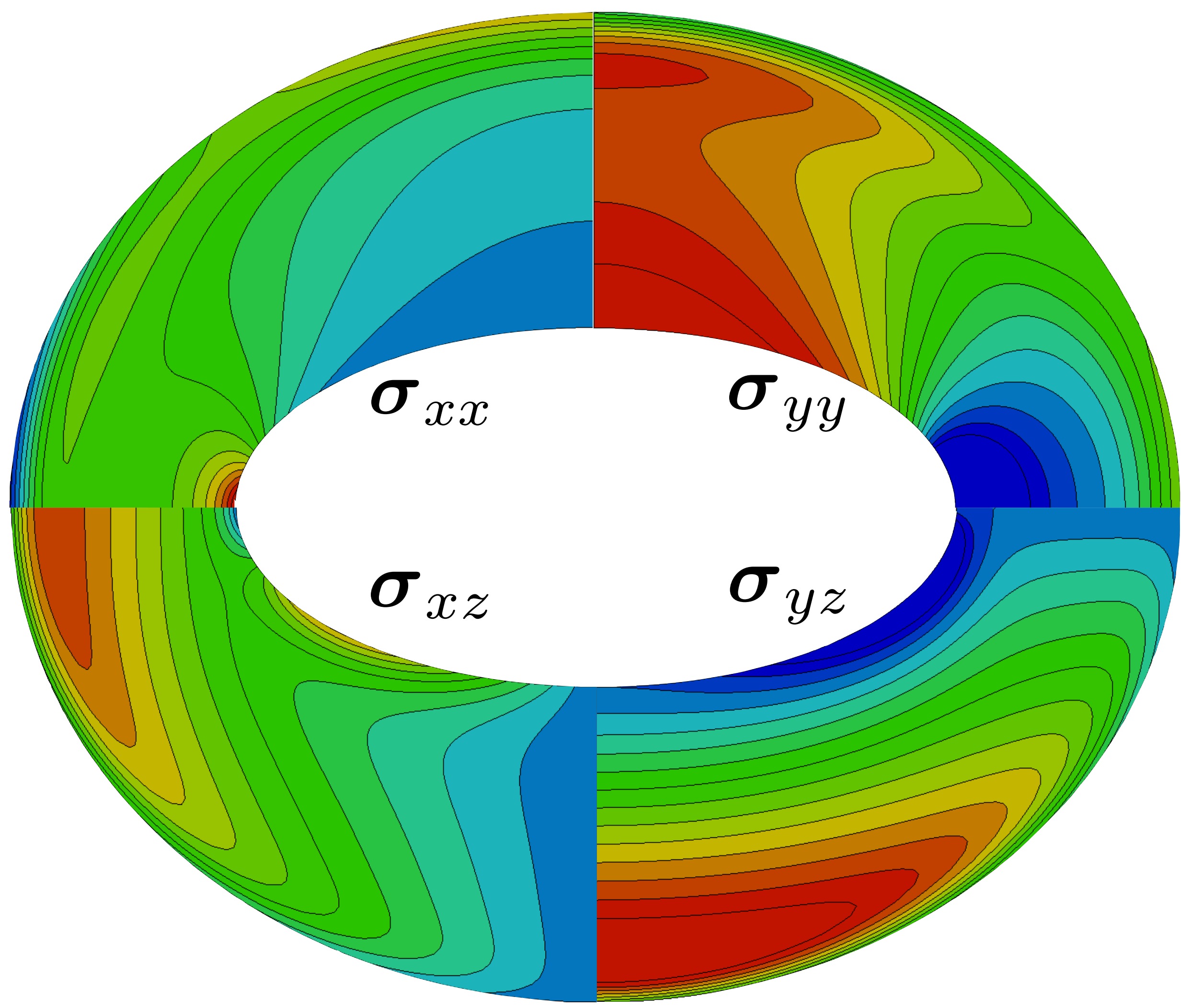

(b) Hexahedral Mesh

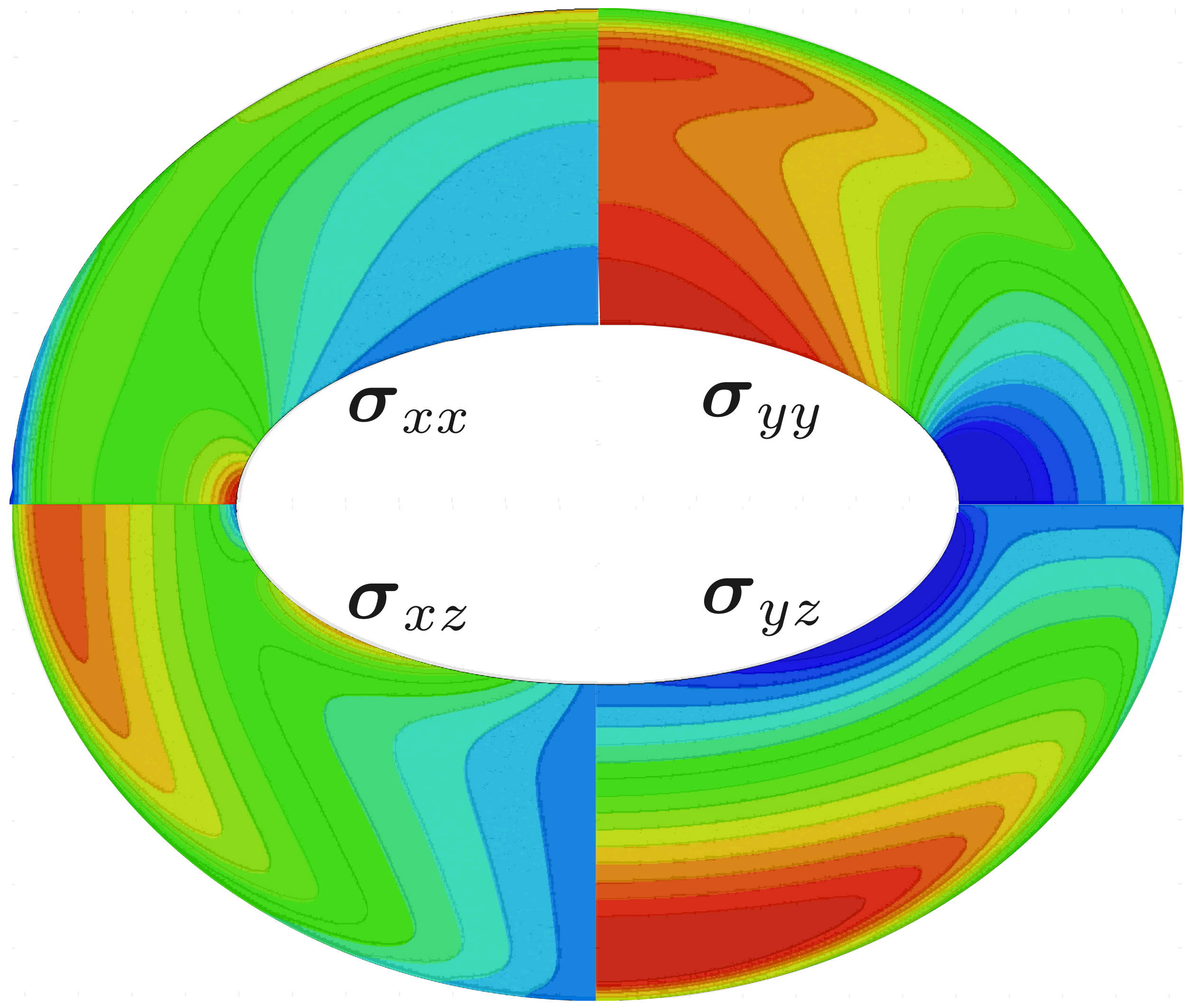

(e) Abaqus (Hexahedral Mesh)

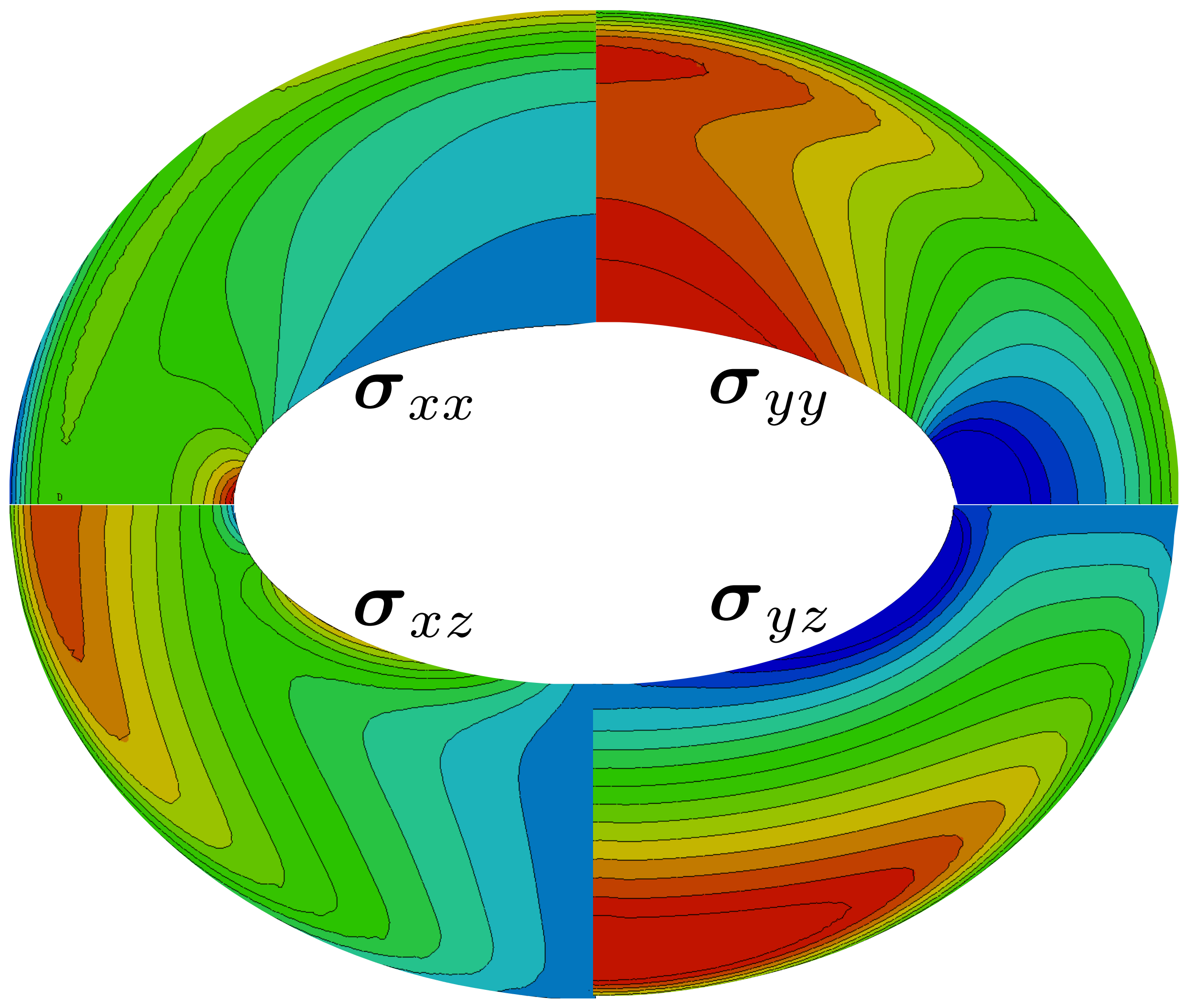

(c) Polyhedral Mesh

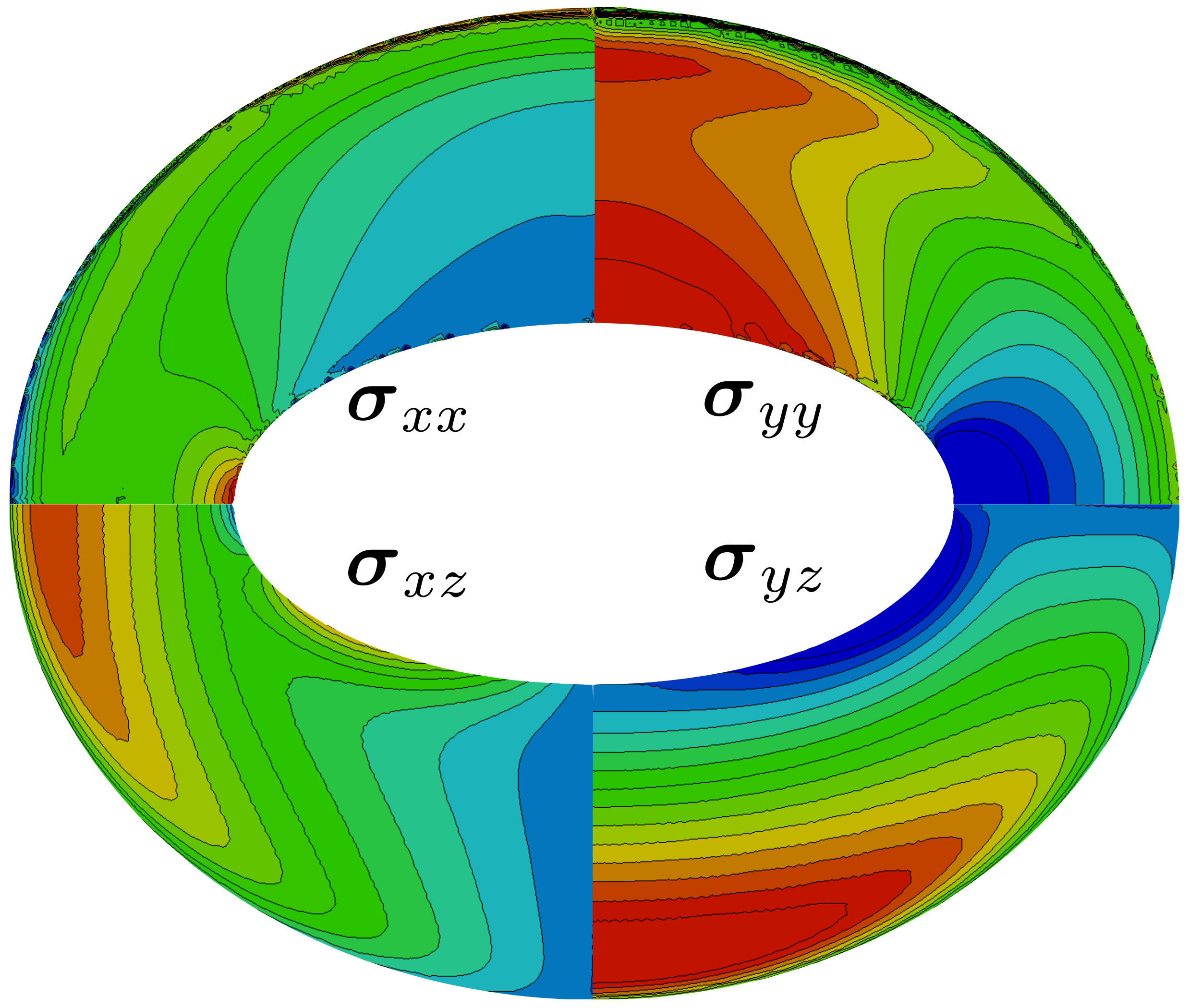

(d) Tetrahedral Mesh

Case 2: Out-of-Plane Bending of an Elliptic Plate

	Coupled		Segregated[1]		Segregated[2]		Abaqus	
Mesh	Time	Memory	Time	Memory	Time	Memory	Time	Memory
72	0.03	7	0.5	6	0.5	6	4	24
576	0.15	13	1	8	2	9	5	31
4 608	1.6	51	6.5	20	14	30	6	107
36 864	11	300	102	80	145	120	34	1 197
294 912	242	2 200	1 474	500	1 990	800	1 375	17 900

Table II. Elliptic plate: wall-clock time (in s) and maximum memory usage (in MB)

Narrow T-section Component

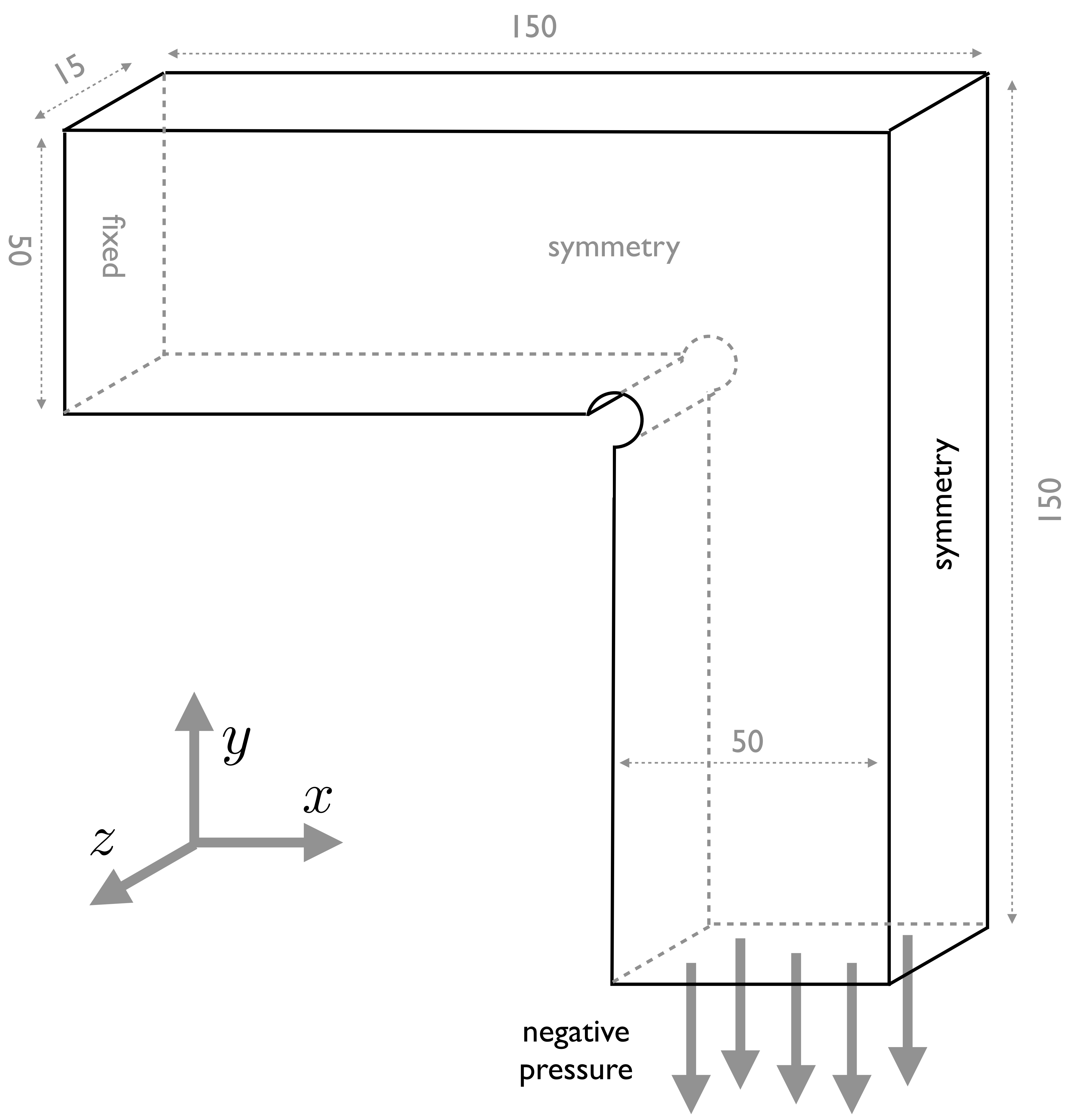

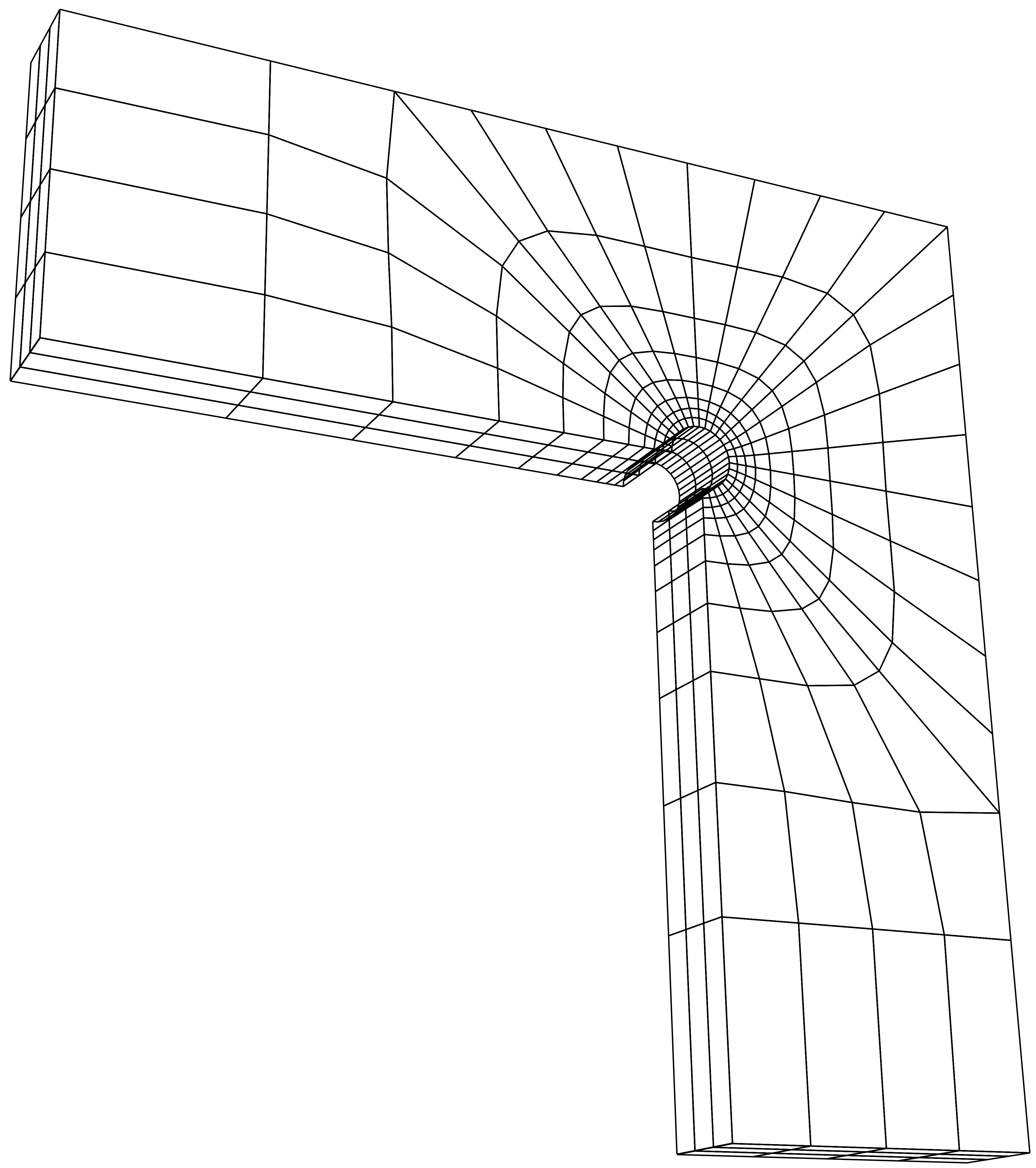

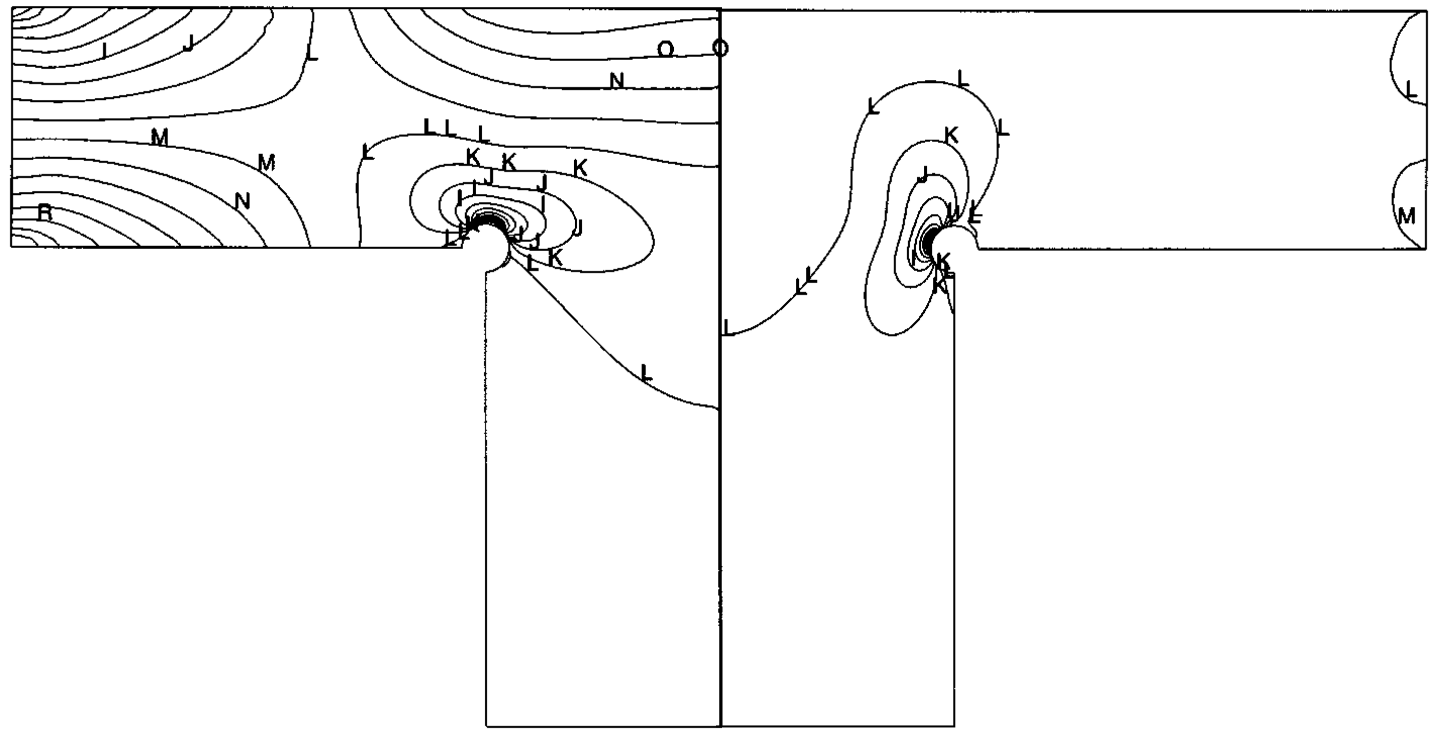

(a) Demirdžić et al. [3] Benchmark

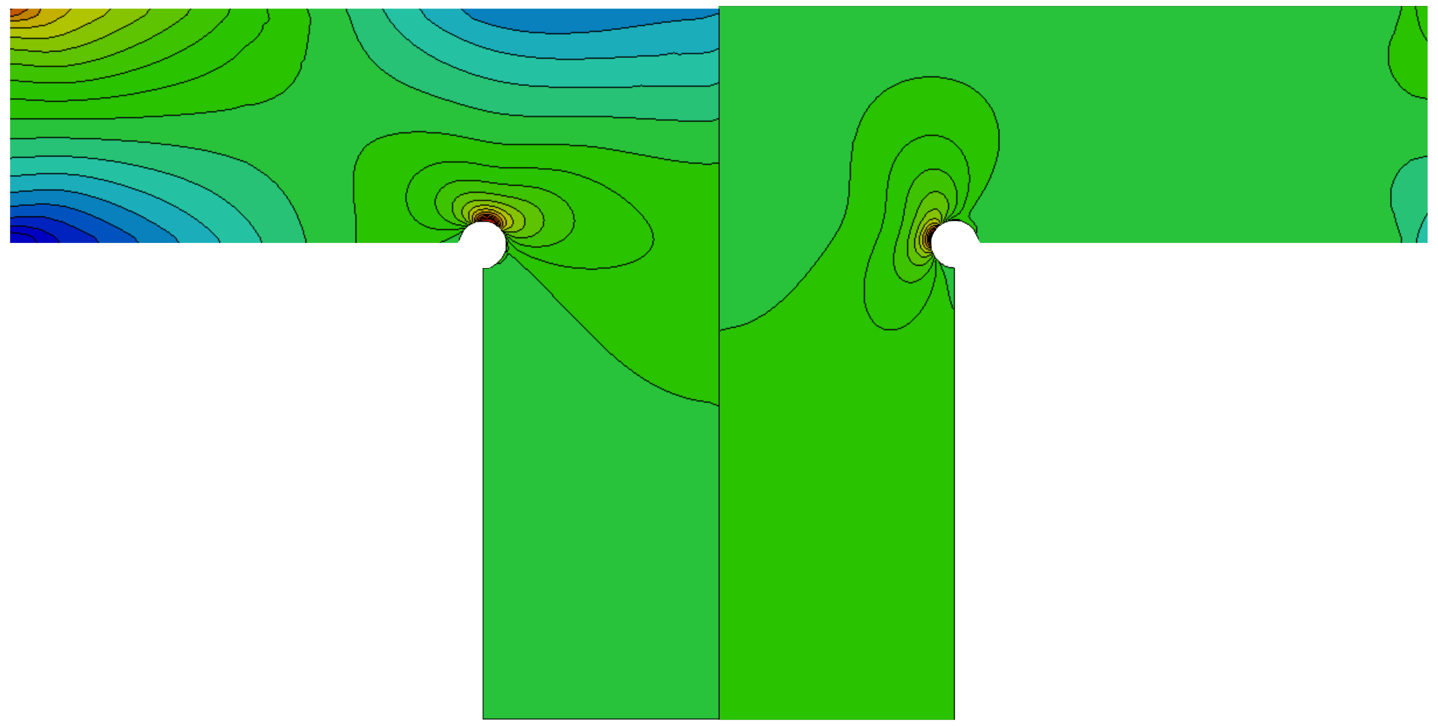

(b) Hexahedral Mesh

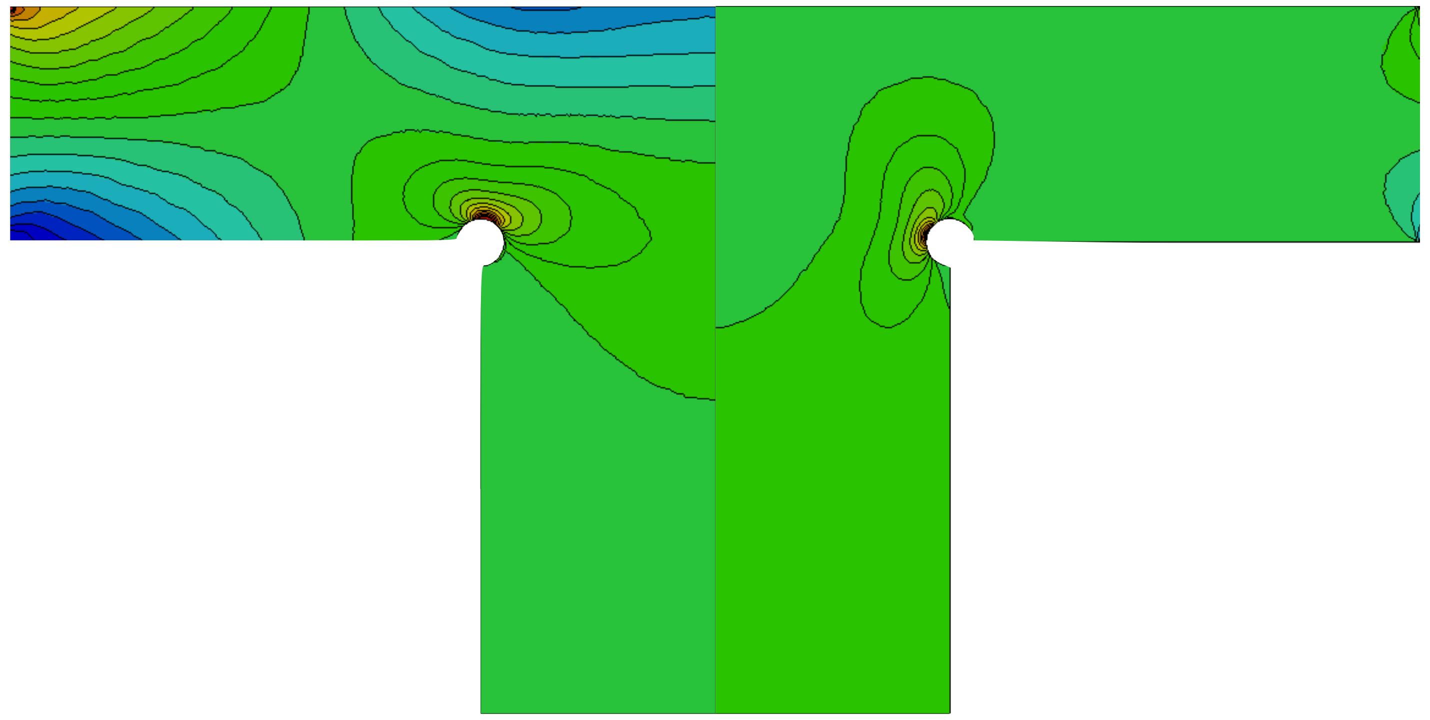

(c) Polyhedral Mesh

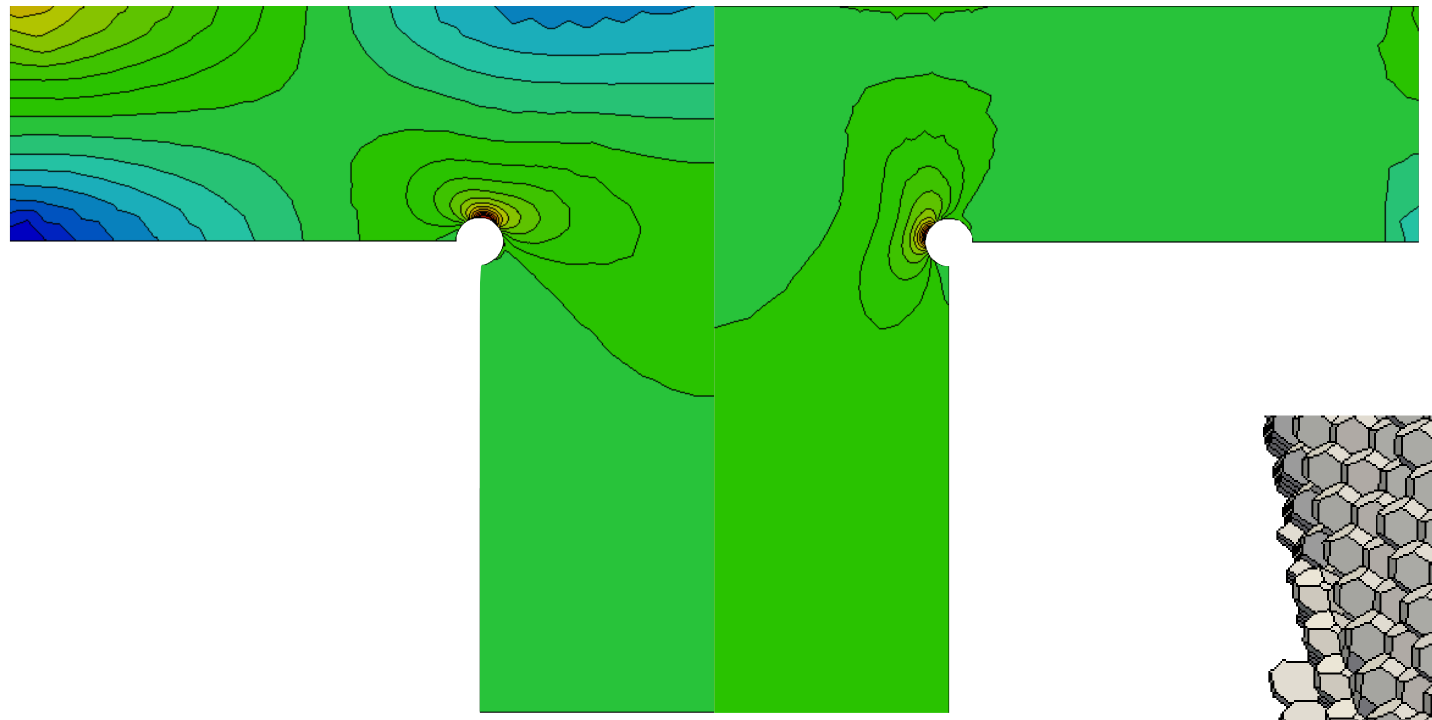

(d) Tetrahedral Mesh

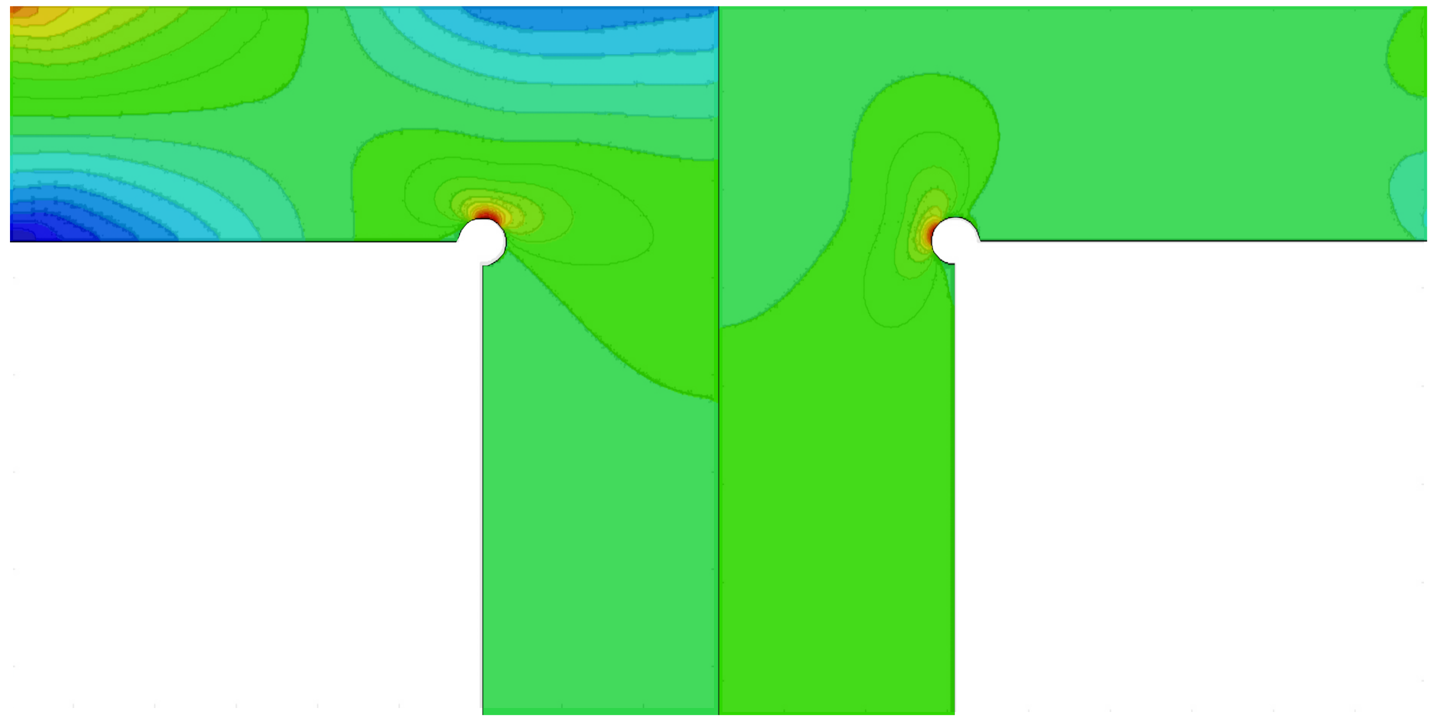

(e) Abaqus Hexahedral Mesh

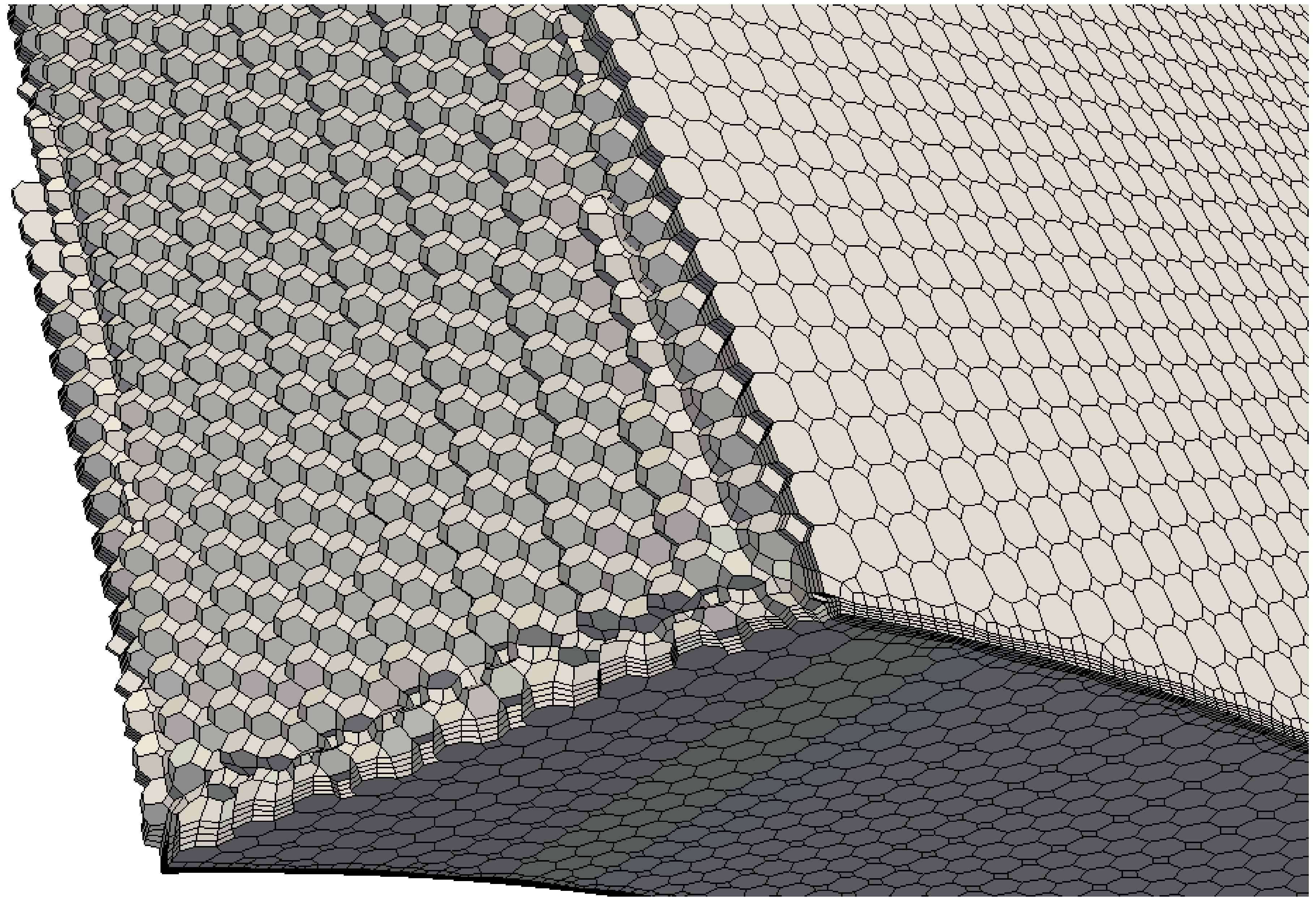

Narrow T-section Component

	Coupled		Segregated[1]		Segregated[2]		Abaqus	
Mesh	Time	Memory	Time	Memory	Time	Memory	Time	Memory
624	0.2	15	0.7	8	1.5	10	2	98
4 992	2	58	6	24	10	30	3	102
39 936	29	340	98	88	416	140	33	1 500
319 488	421	2 400	2 220	560	2 647	900	1 236	13 000

Table III. Narrow T-section component: wall-clock time (in s) and maximum memory usage (in MB)

*See article almost in press *fingers crossed*:*

P. Cardiff, Z. Tukovic, H. Jasak, and A. Ivankovic, "**A block-coupled finite volume methodology for linear elasticity and unstructured meshes**," Computers and structures, 2016, *revision under review*.

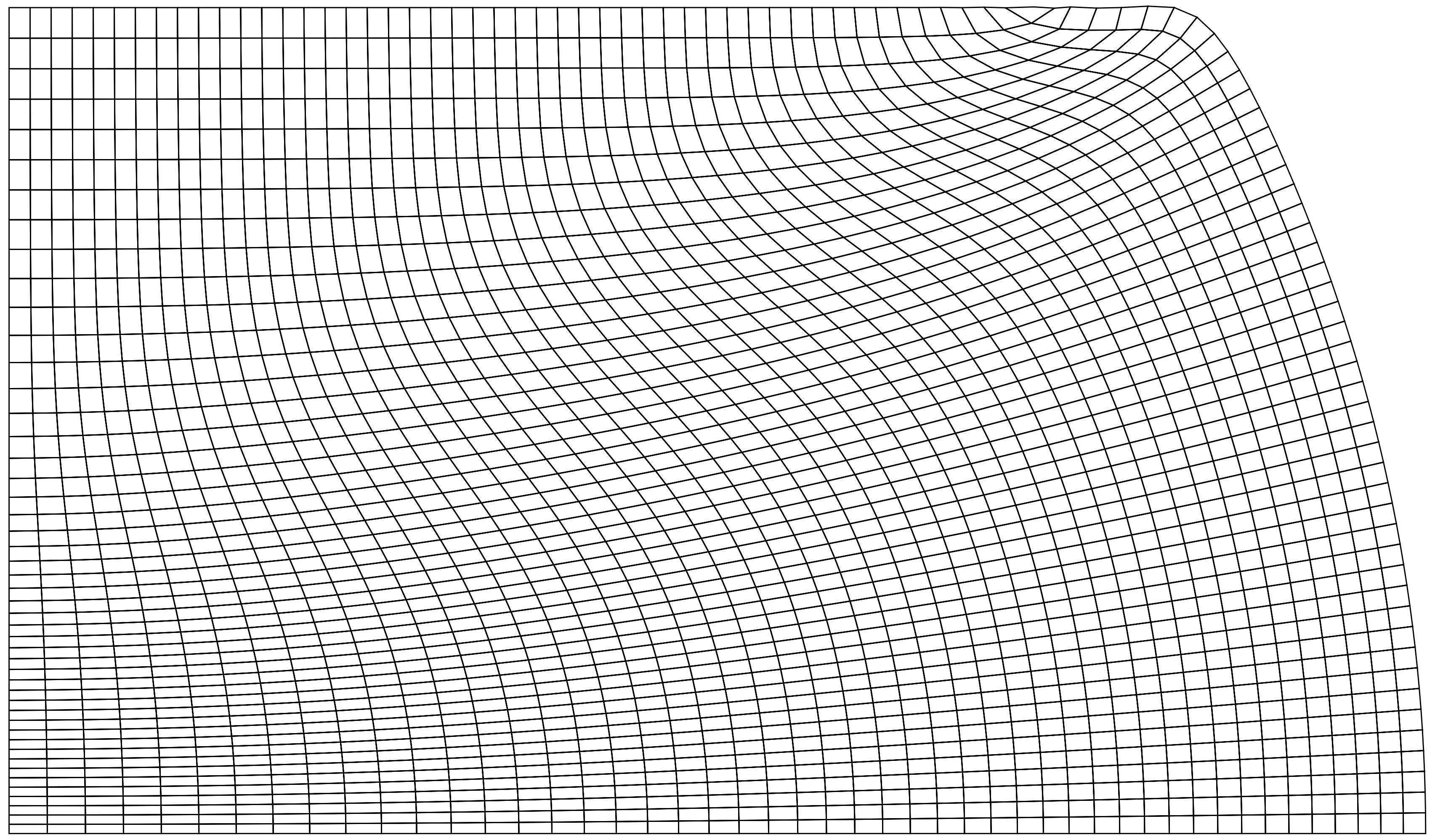

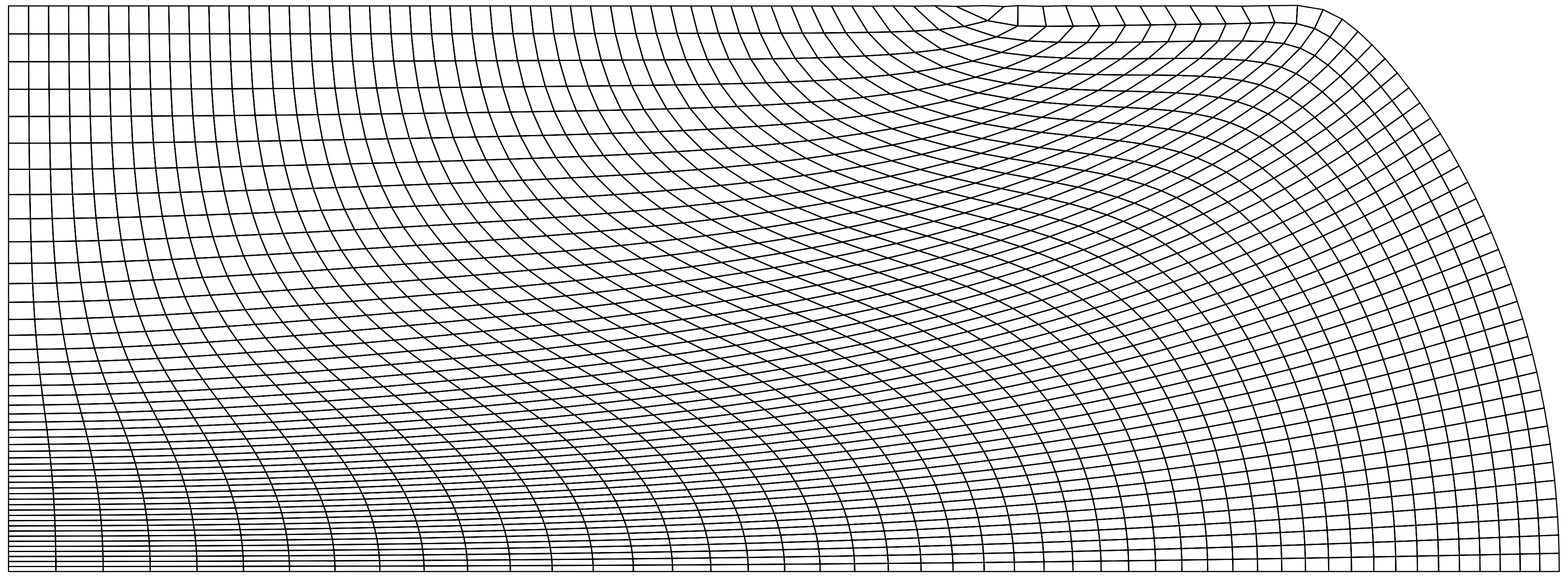

Nonlinear Benchmark Cases

Upsetting a billet

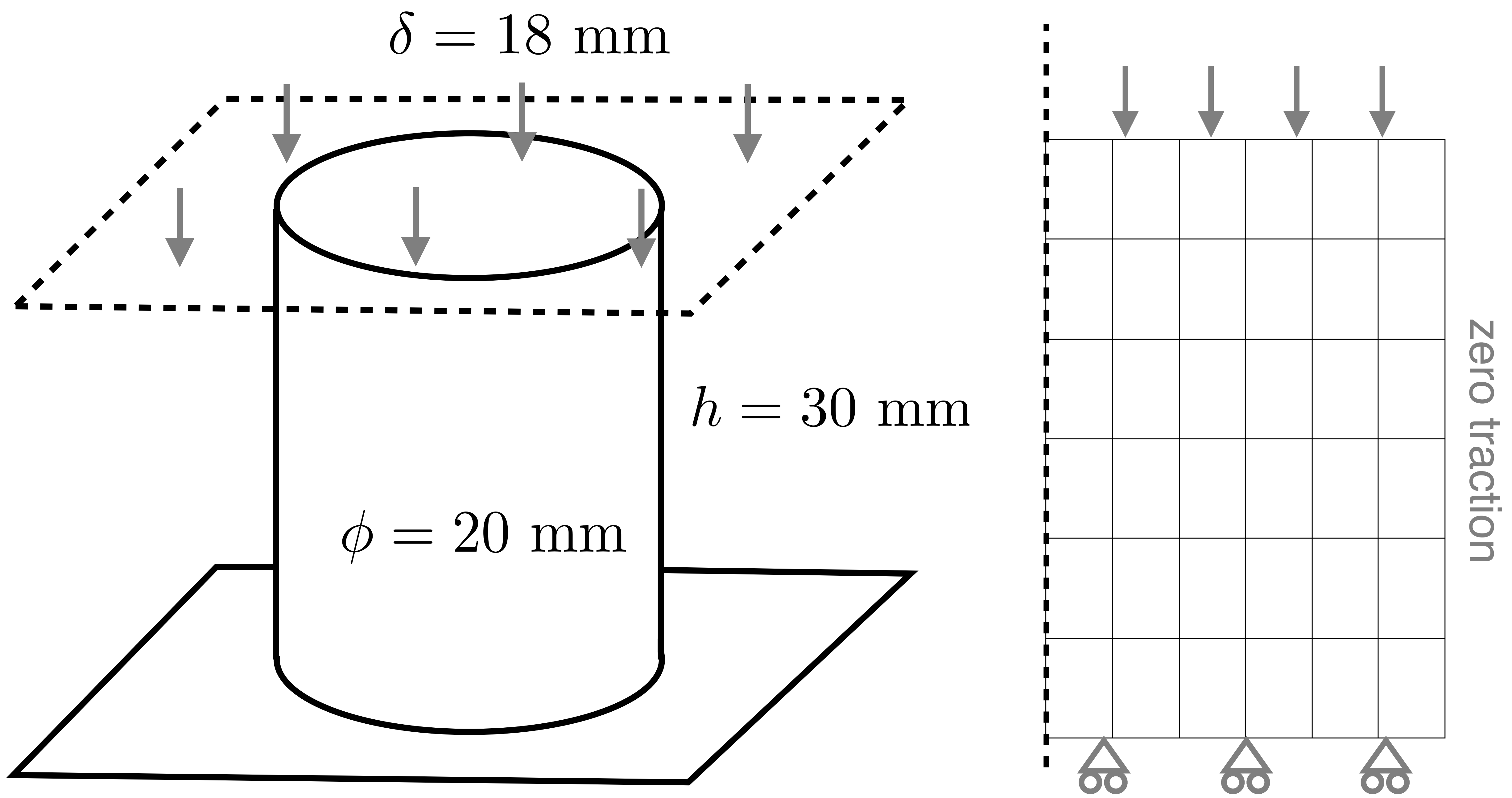

(a) Geometry (b) 2-D axisymmetric mesh

Young's modulus	E	200 GPa
Poisson's ratio	ν	0.3
Initial yield stress	σ_Y	700 MPa
Hardening parameter	κ	300 MPa

See ***other*** *article almost in press *fingers crossed*:*

P. Cardiff, Z. Tukovic, P. De Jaeger, M. Clancy and A. Ivankovic, "**A Lagrangian cell-centred finite volume method for metal forming simulation**," International journal for numerical methods in engineering, 2016, *revision under review*.

Upsetting a billet

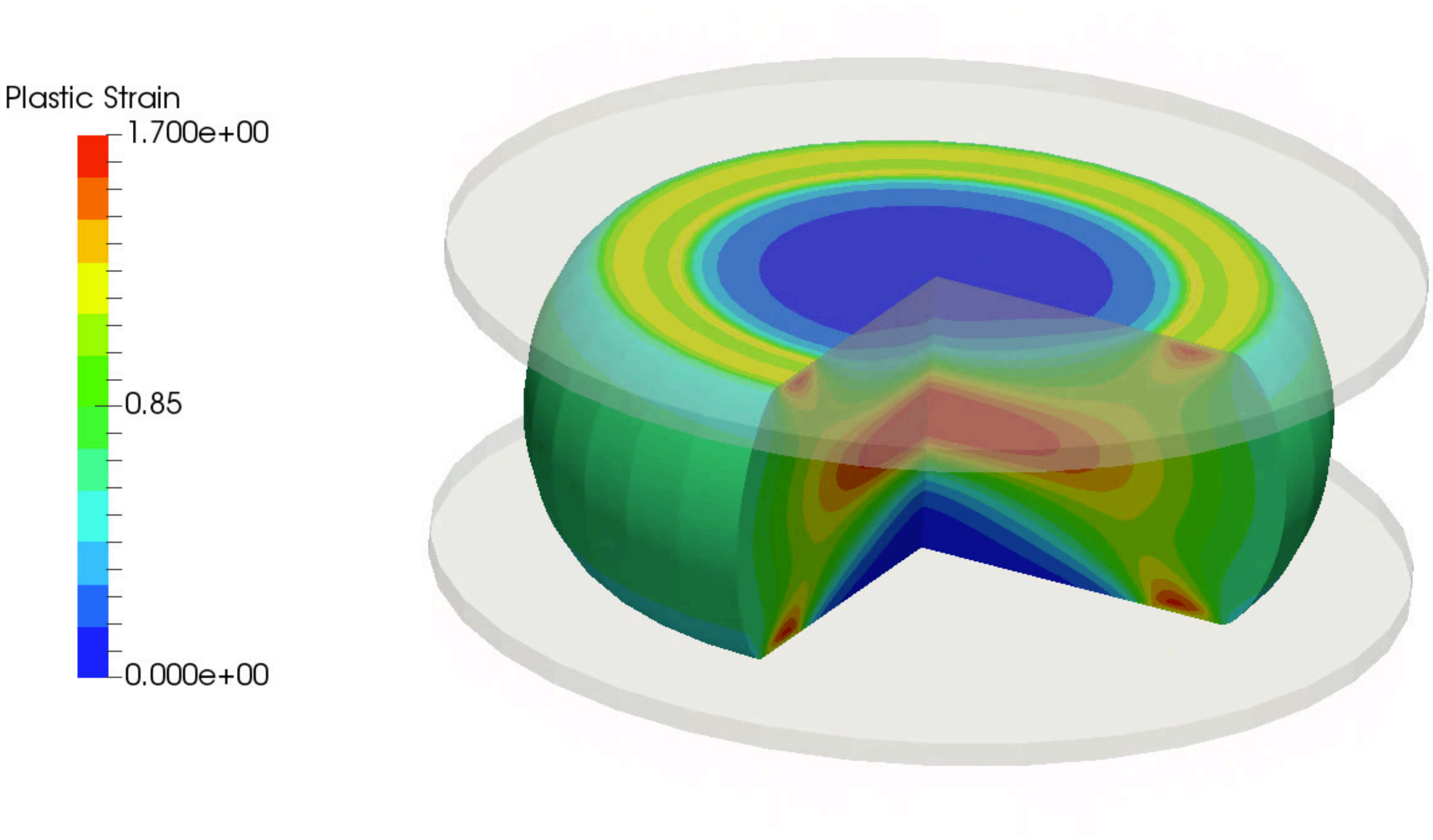

Precent upset: 60.0

Philip Cardiff
UCD

Upsetting a billet

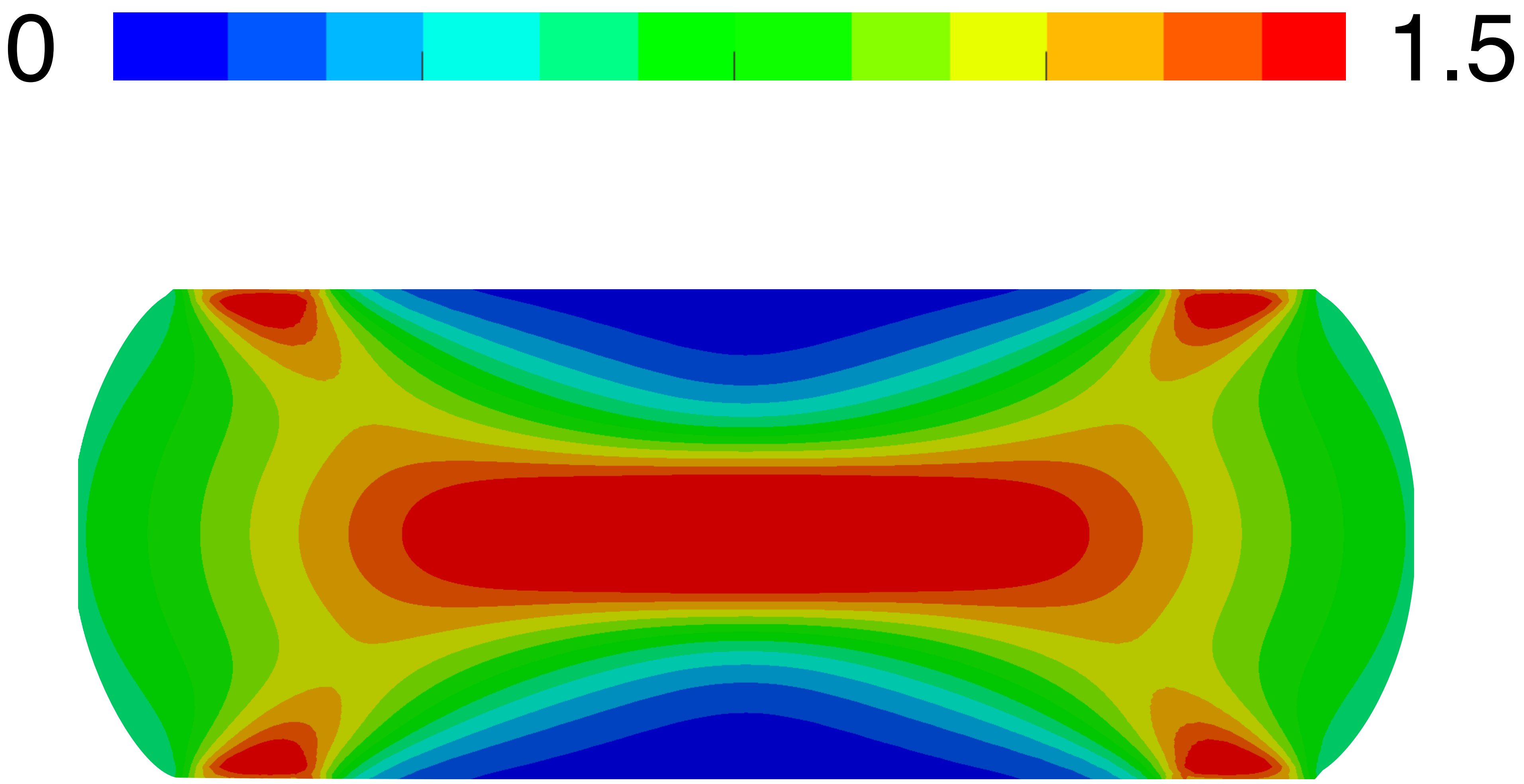

OpenFOAM vertex-wise

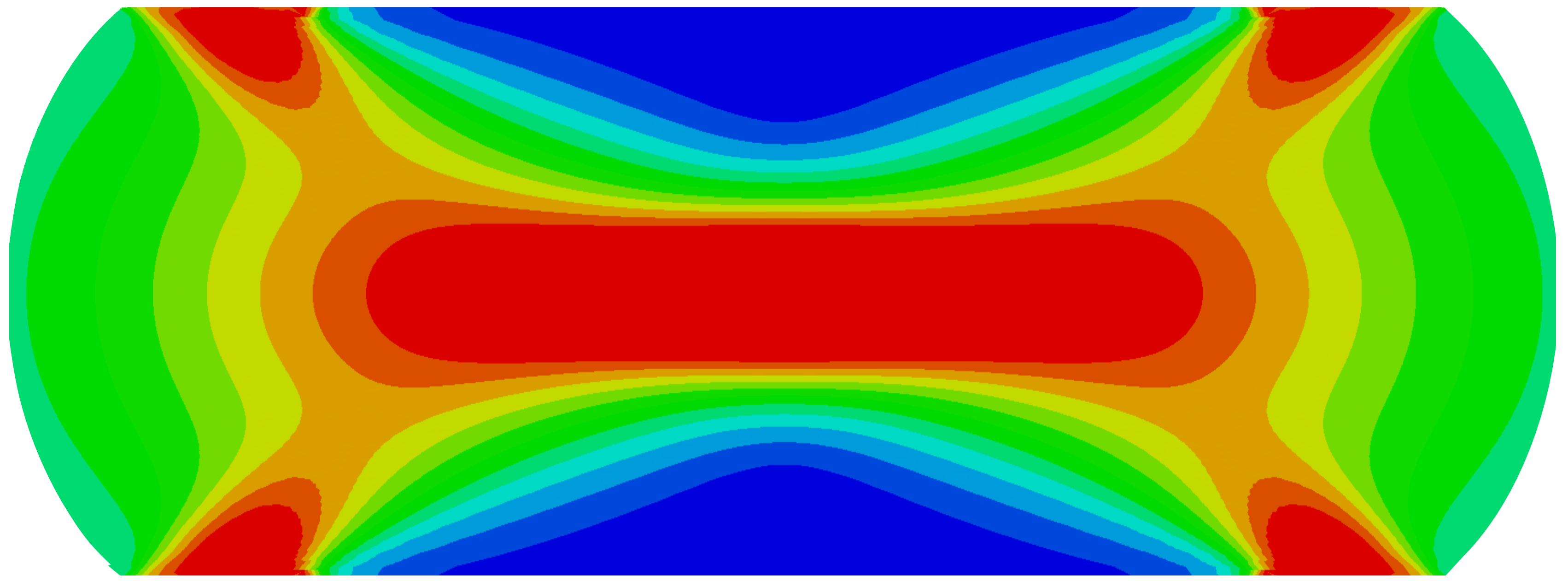

Abaqus

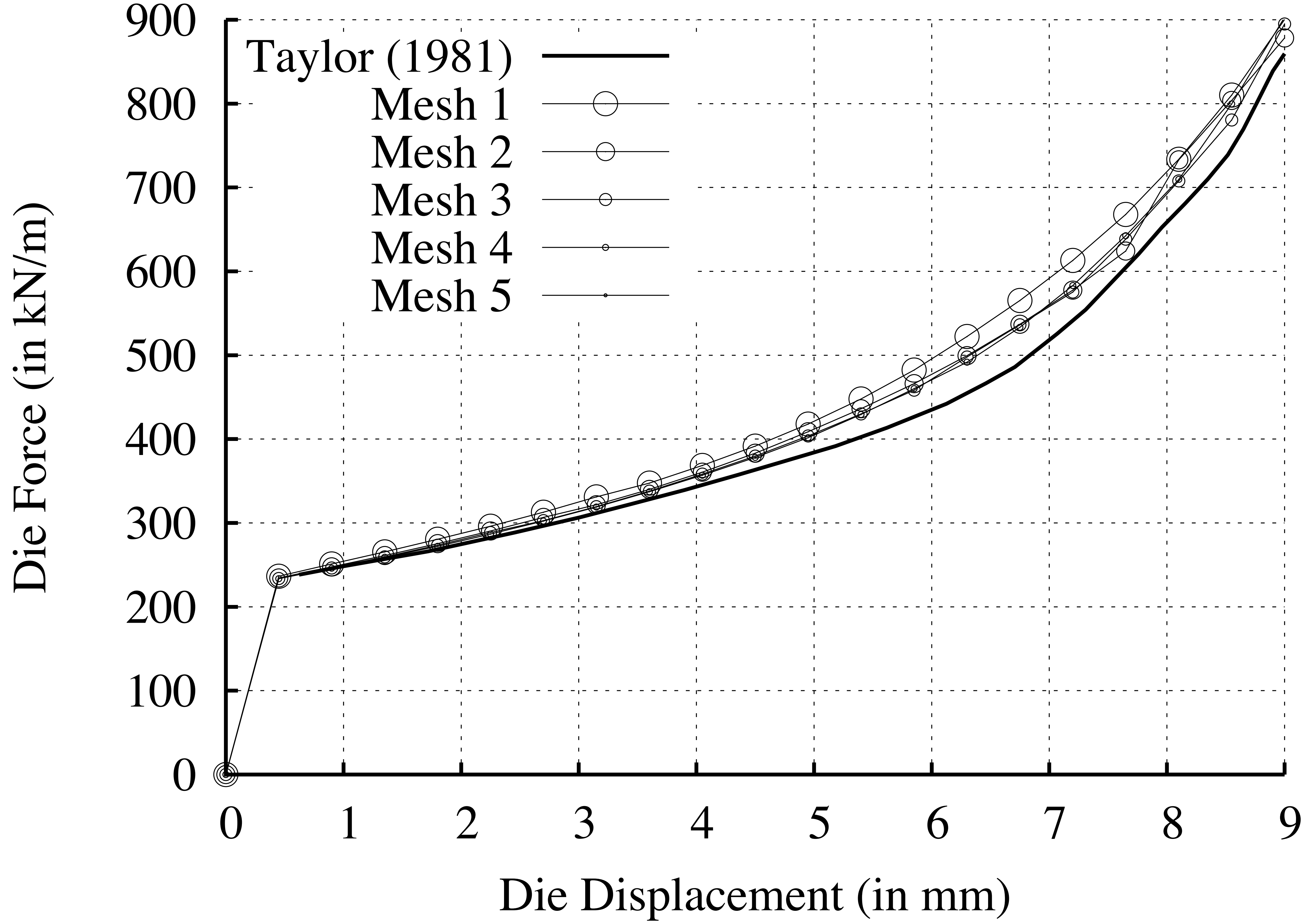

Crushing a pipe

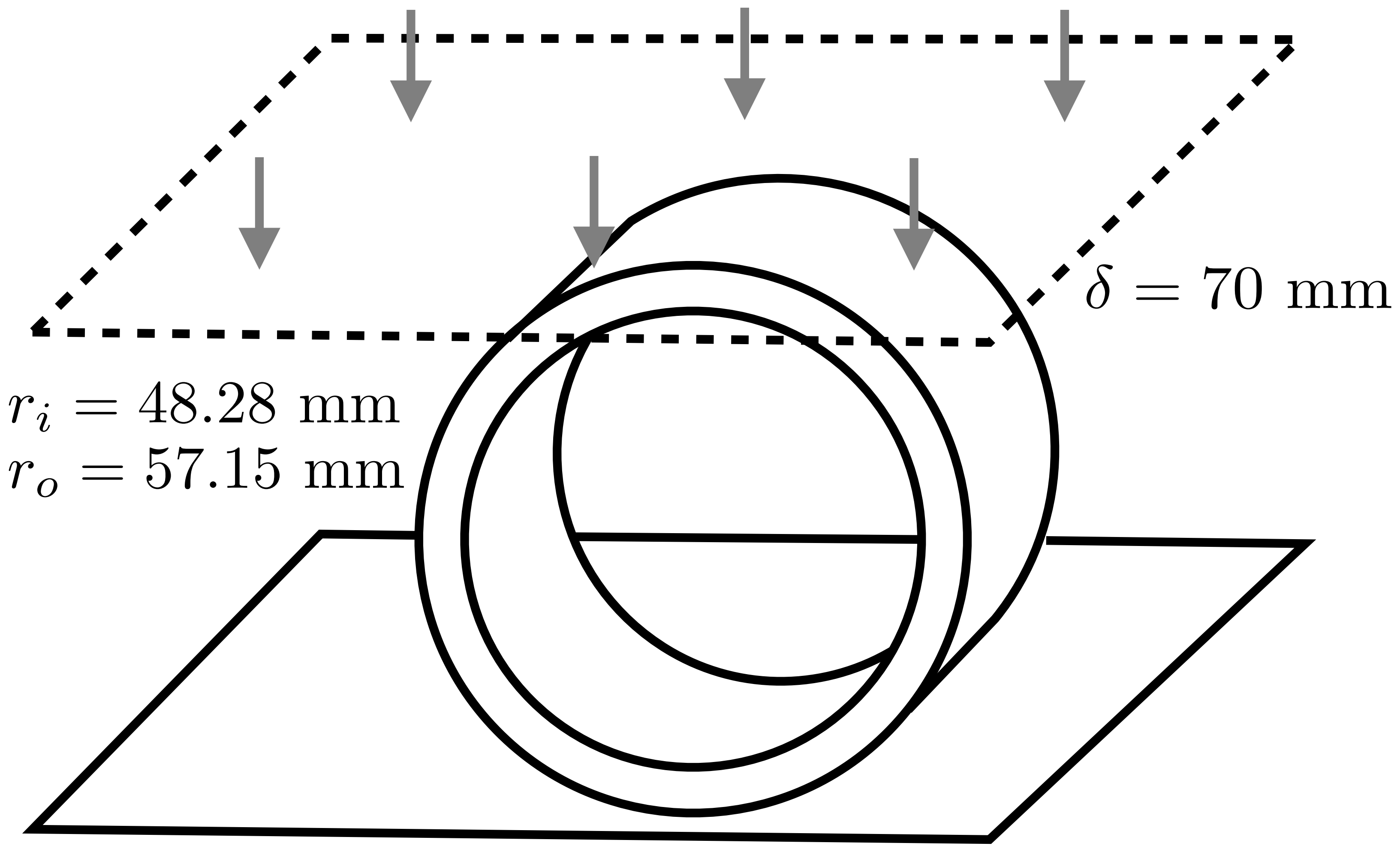

(a) Geometry

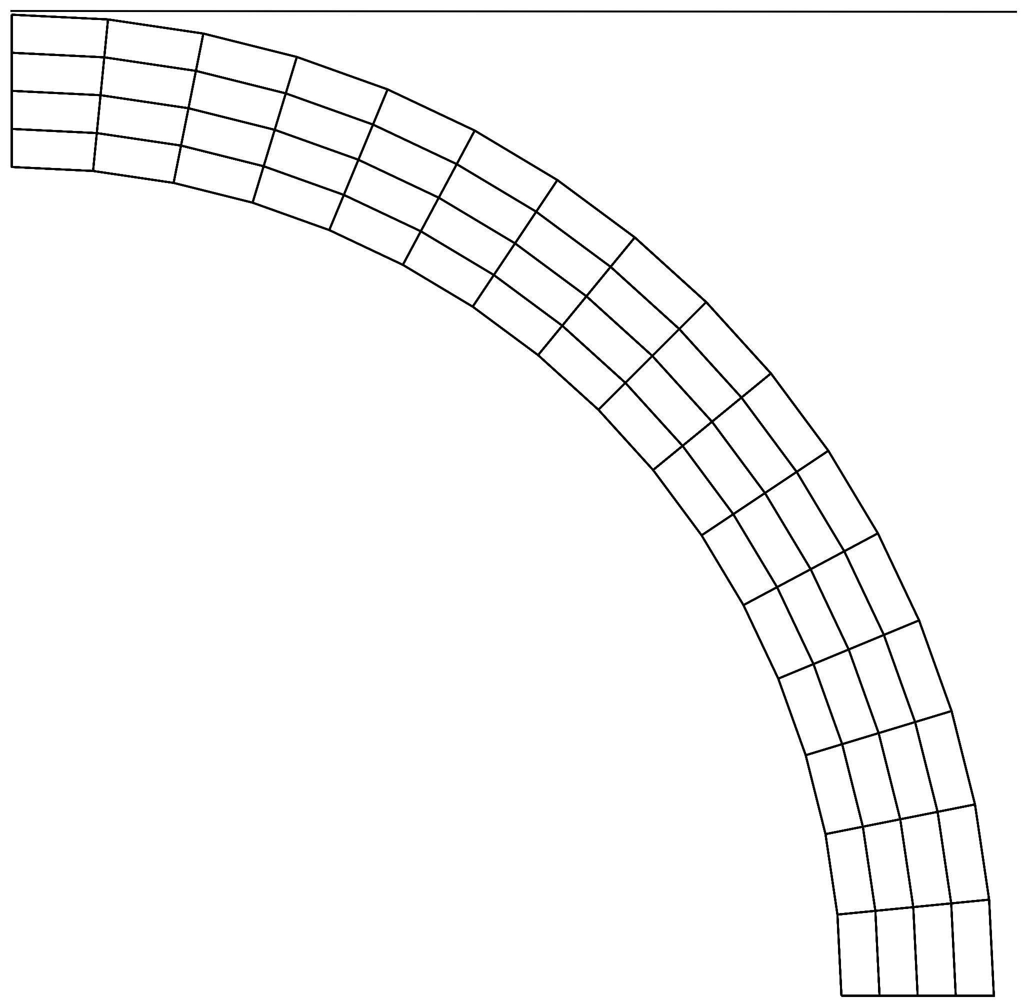

(b) 2-D Plane Strain Mesh

Young's modulus	E	186 GPa
Poisson's ratio	ν	0.3
Initial yield stress	σ_Y	241.32 MPa
Hardening	Plastic strain	Yield stress (in MPa)
	0	241.32
	0.0035	275.79
	0.0083	301.65
	0.0133	318.88
	0.0182	344.74
	0.0281	361.98
	0.0380	379.21
	1	1 482.37

Crushing of a pipe

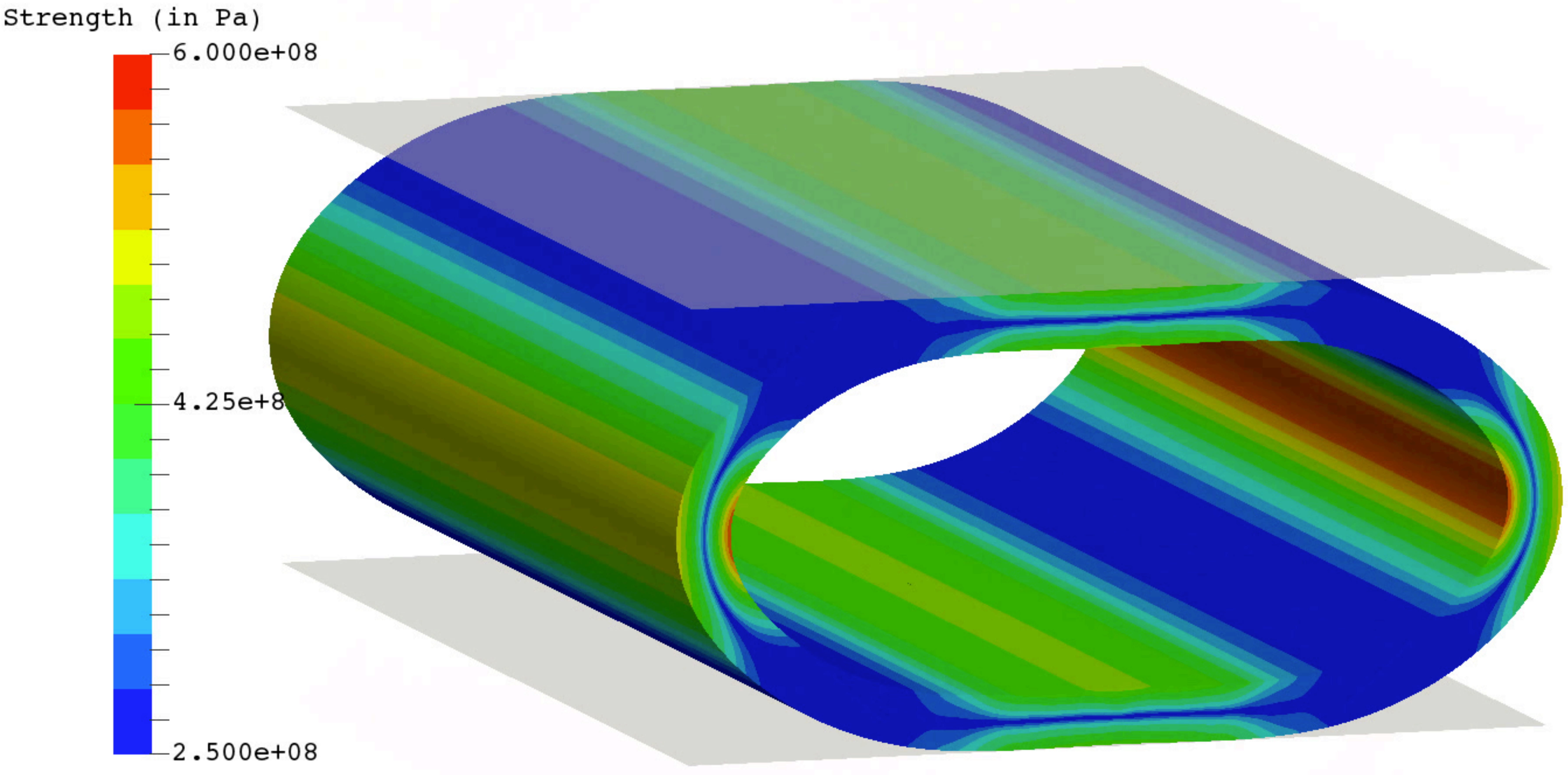

Time: 0.61 s

Philip Cardiff
UCD

Crushing a pipe

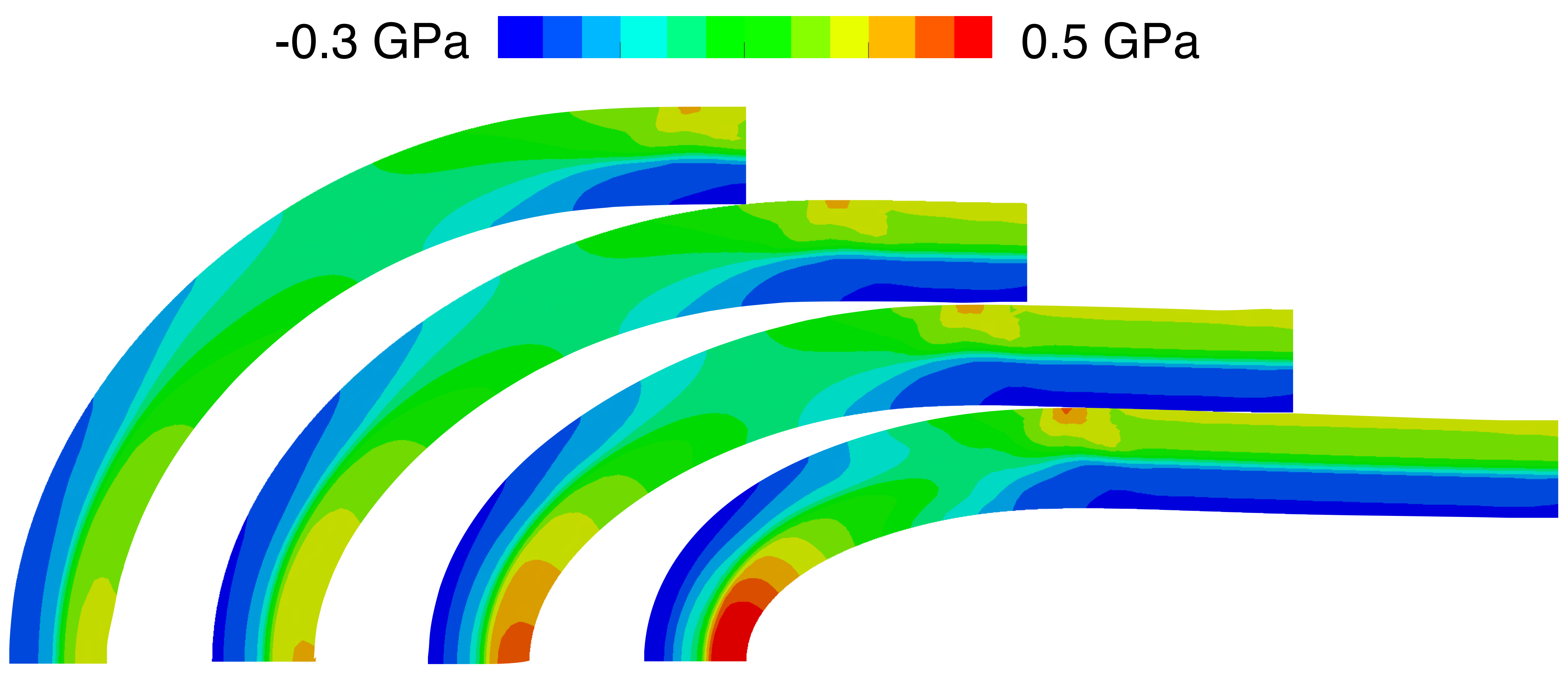

Abaqus

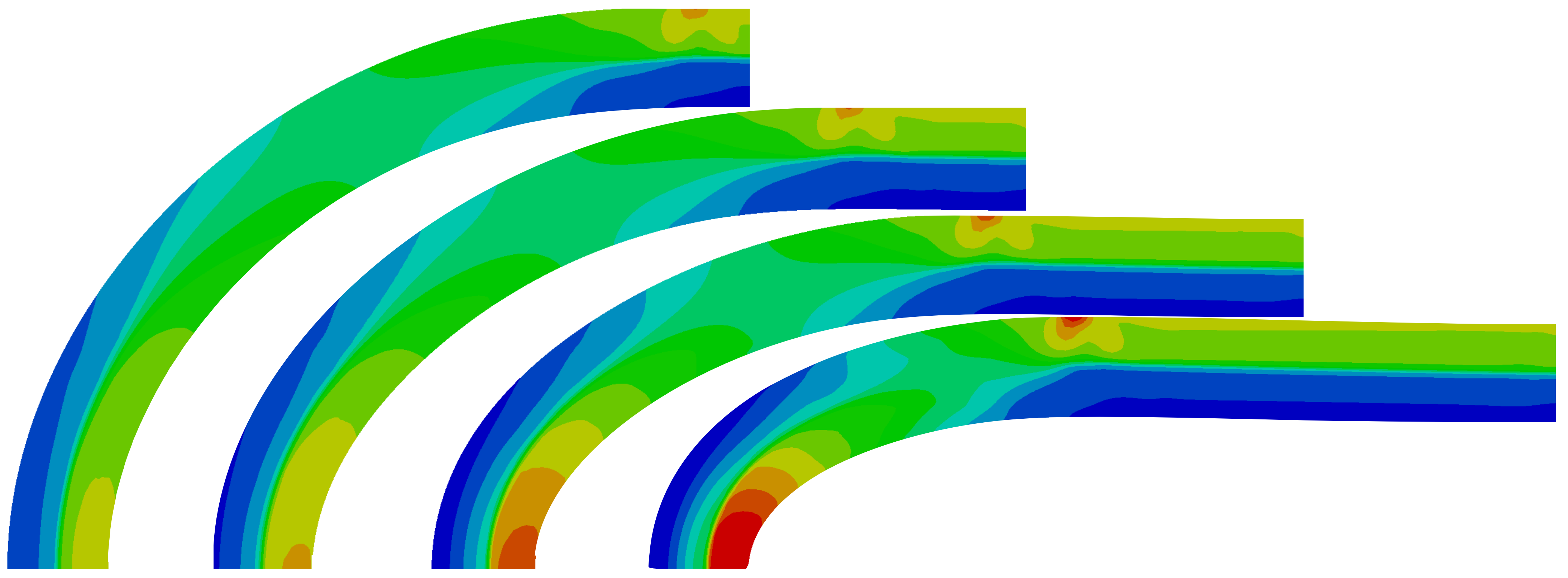

OpenFOAM vertex-wise (modified approach)

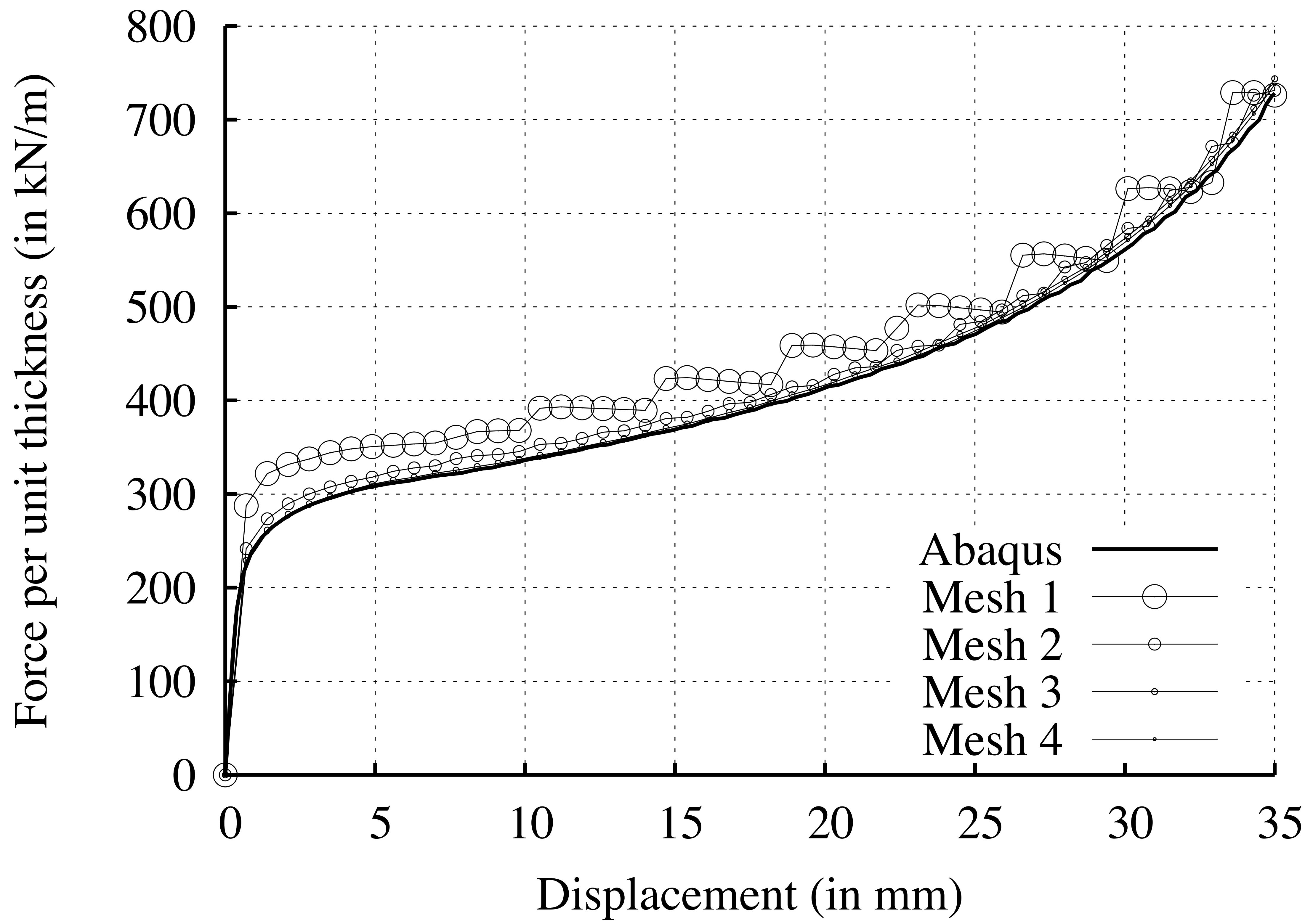

Necking of a bar

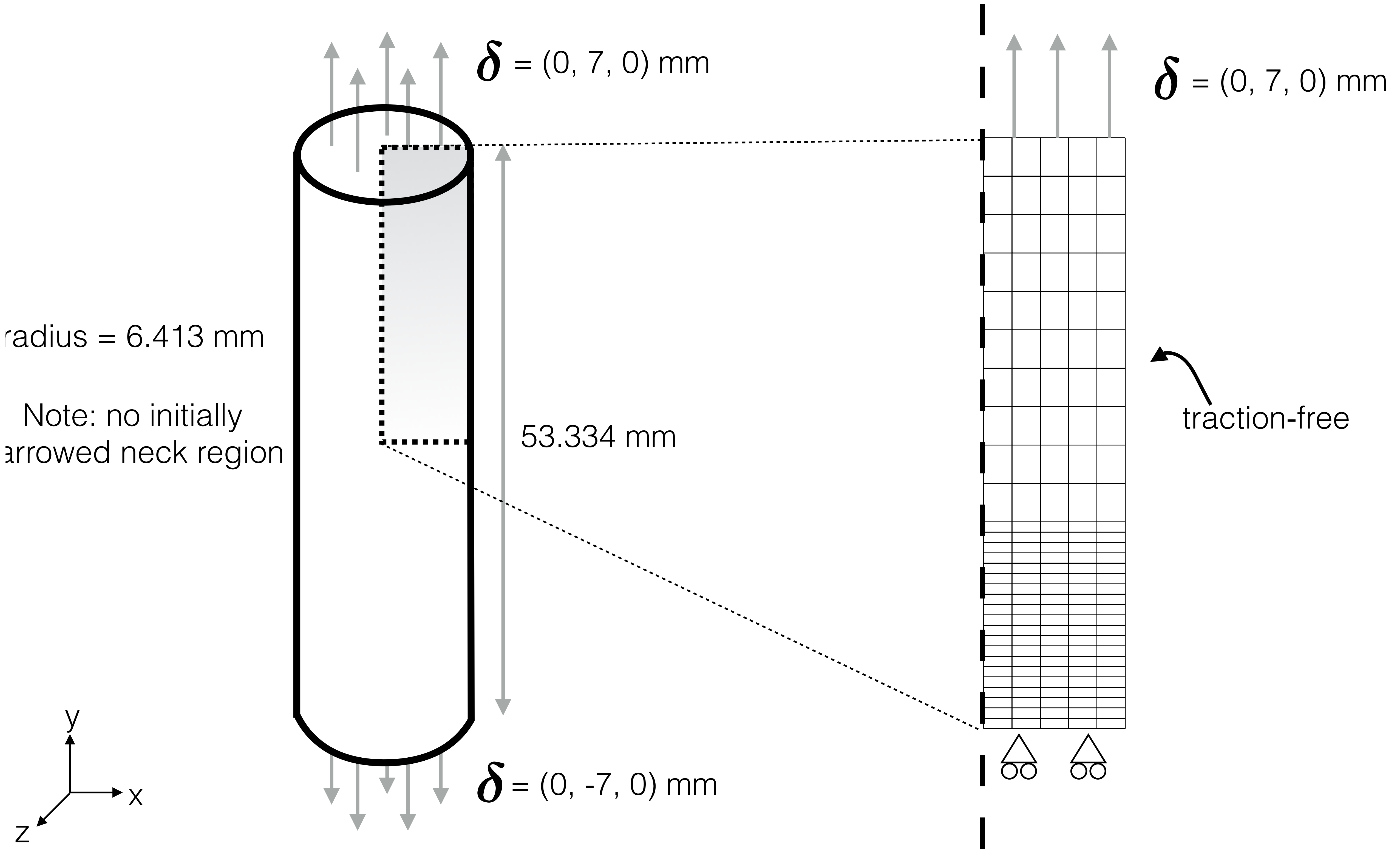

Young's modulus	E	200 GPa
Poisson's ratio	ν	0.3
Initial yield stress	σ_Y	451 MPa
Hardening	Plastic strain	Yield stress (in MPa)
	0.000	451
	0.006	476
	0.019	525
	0.038	583
	0.066	642
	0.147	710
	0.500	777
	1.000	831

Necking of a bar

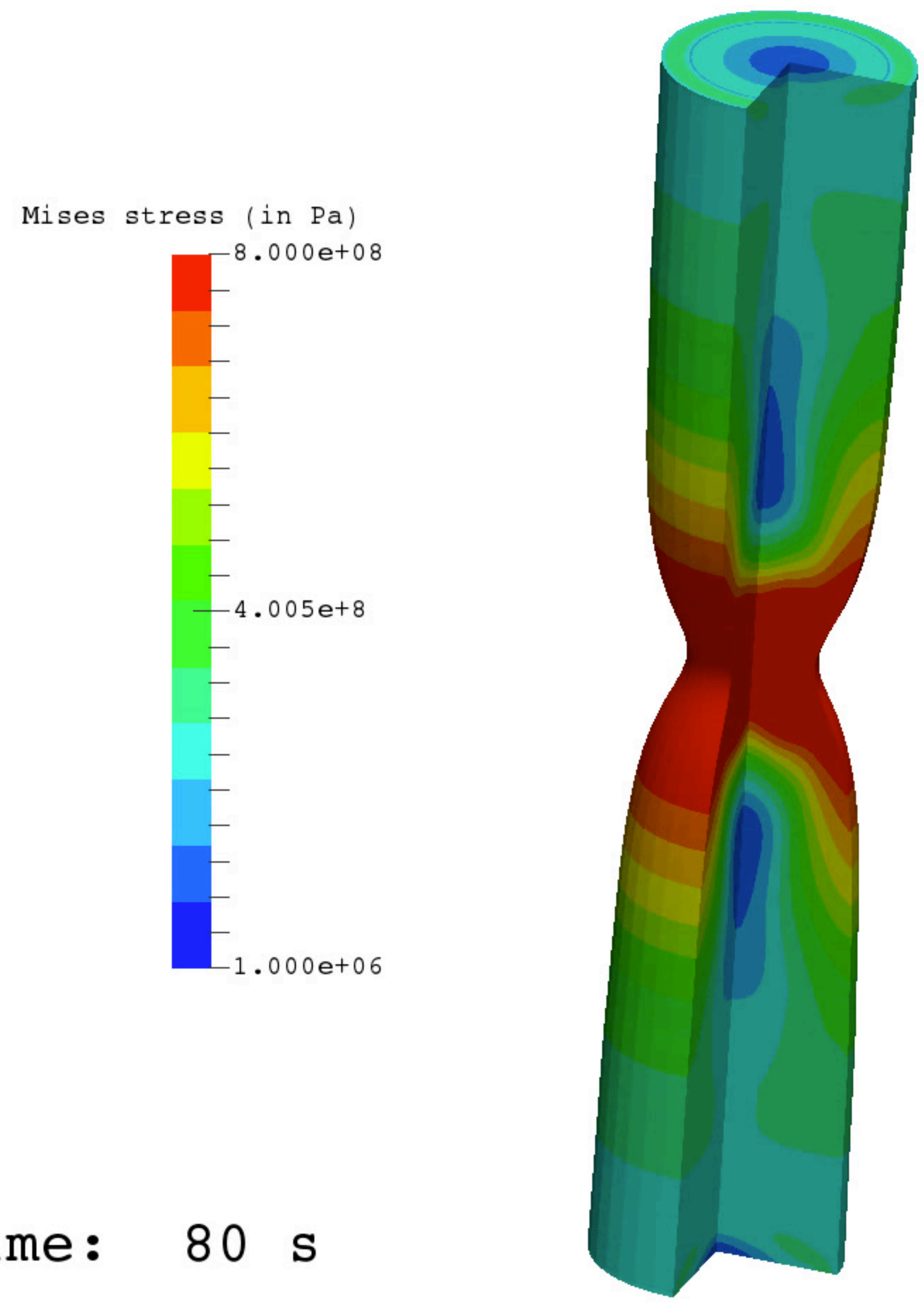

Time: 80 s

Philip Cardiff
UCD

Necking of a bar

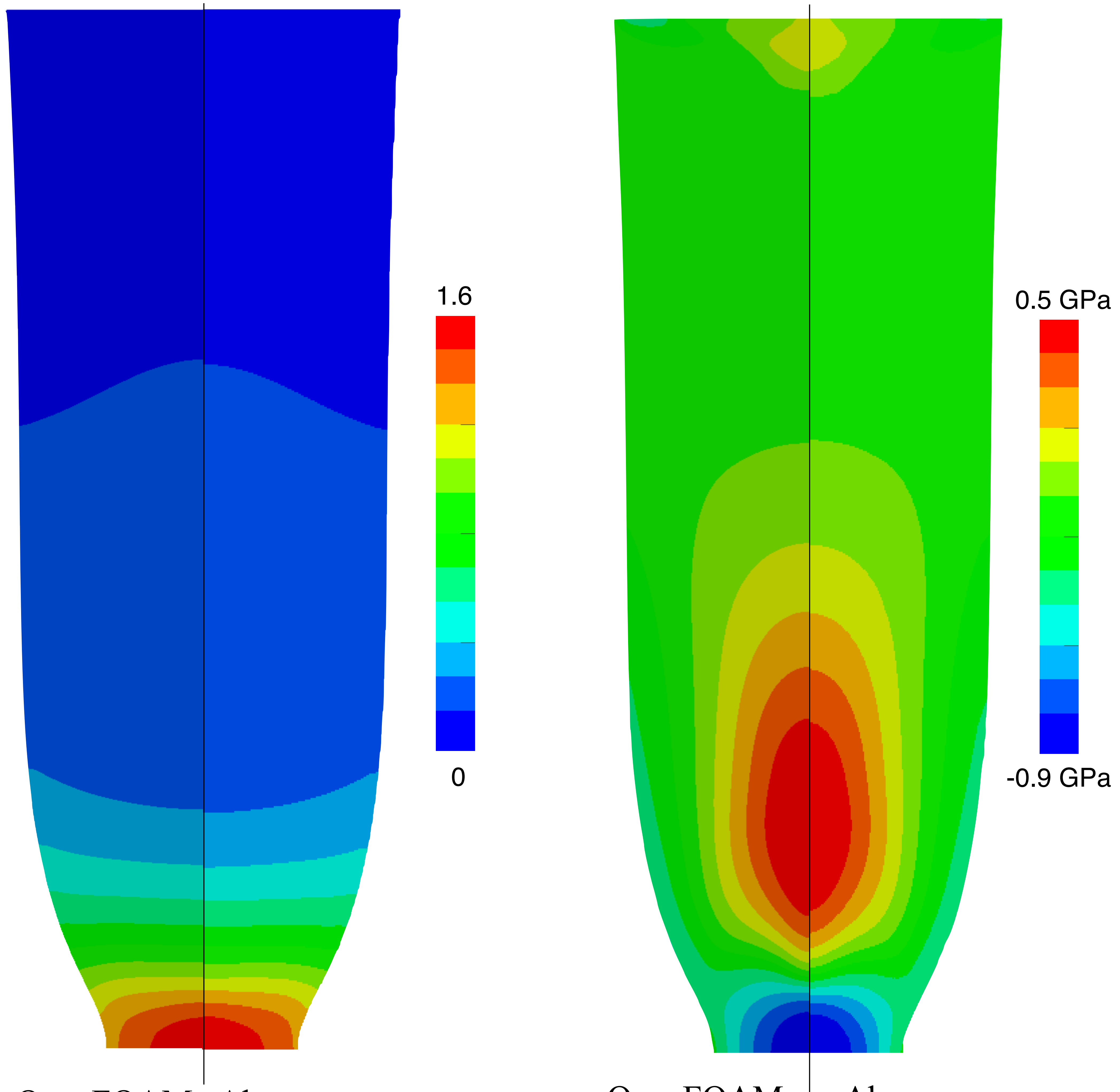

(a) Plastic strain: OpenFOAM FV (left) and Abaqus FE (right)

(b) Pressure: OpenFOAM FV (left) and Abaqus FE (right)

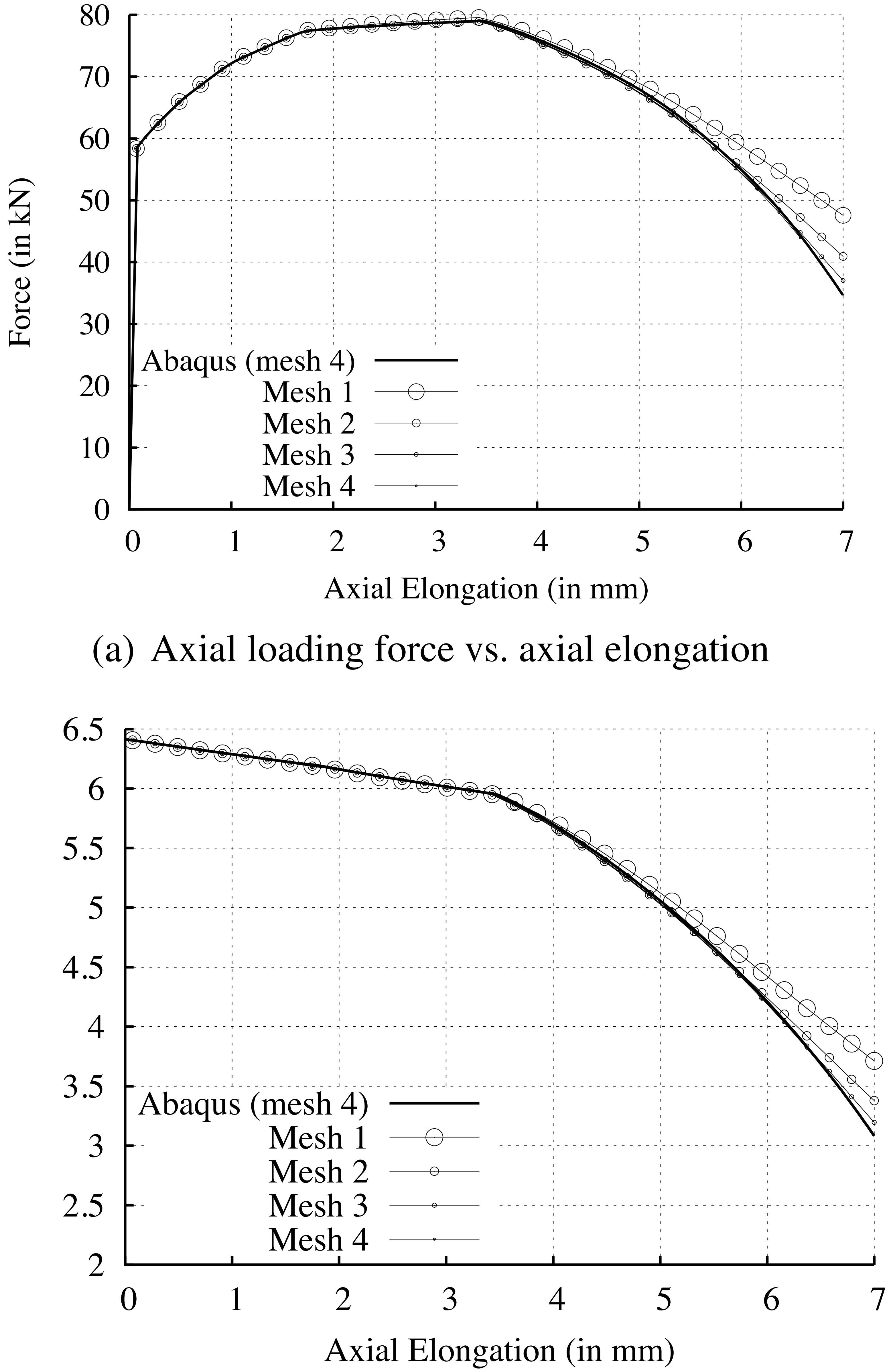

(a) Axial loading force vs. axial elongation

(b) Neck radius vs. axial elongation

Impacting bar

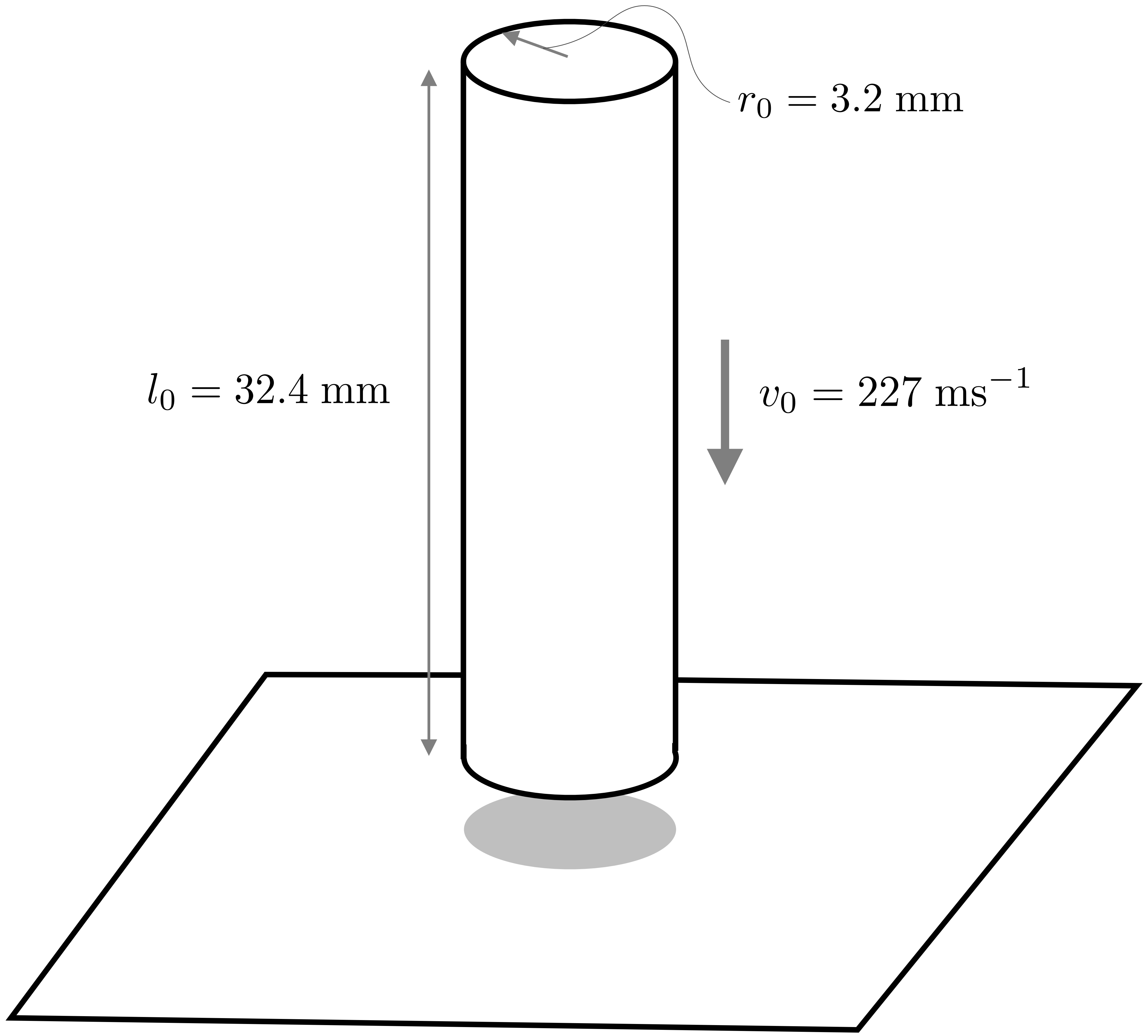

Initial density	ρ	8930 kg/m^3
Young's modulus	E	117 GPa
Poisson's ratio	ν	0.35
Initial yield stress	σ_Y	400 MPa
Hardening modulus	κ	100 MPa

High speed billet impact

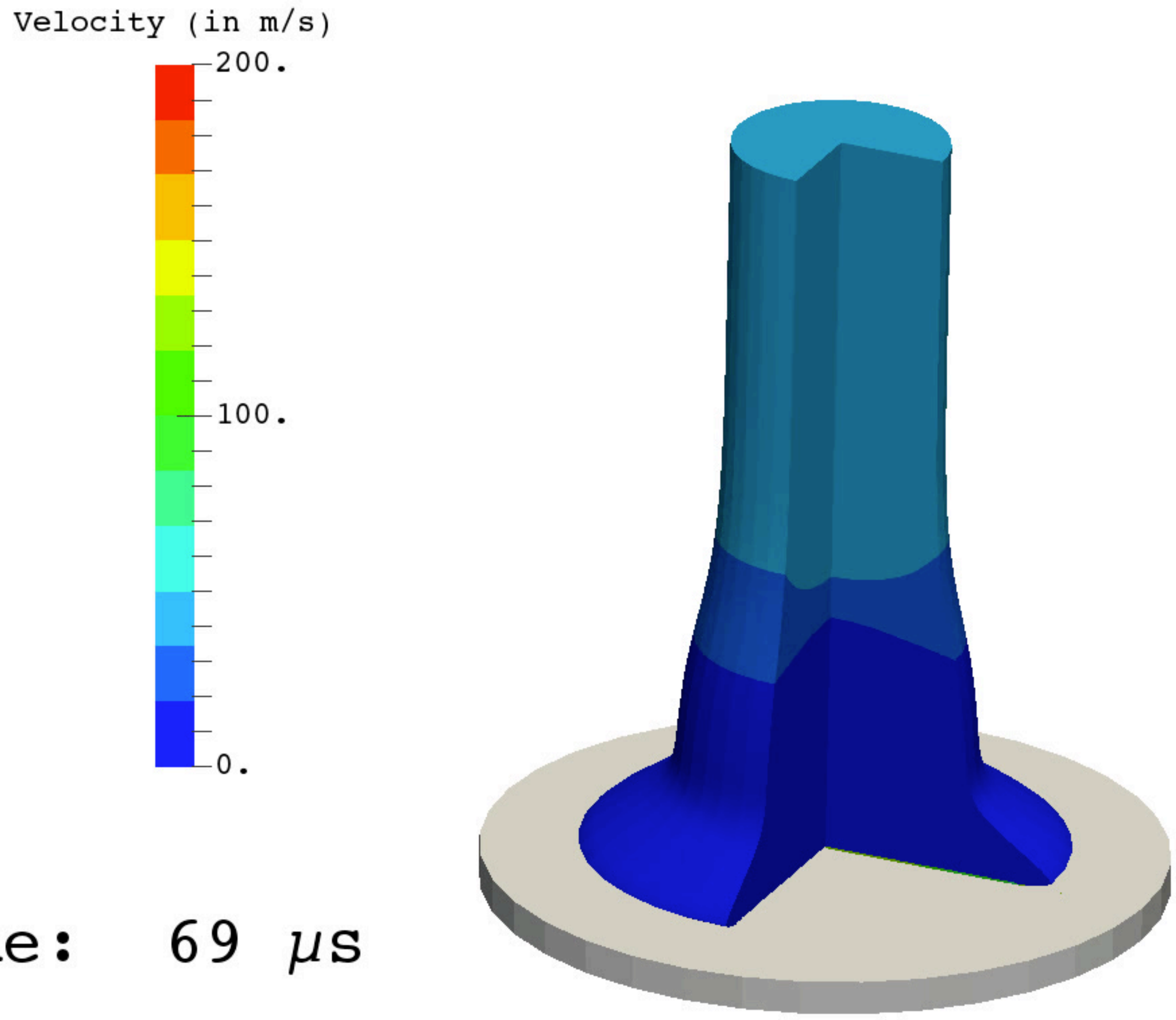

Time: 69 μs

Philip Cardiff
UCD

Impacting bar

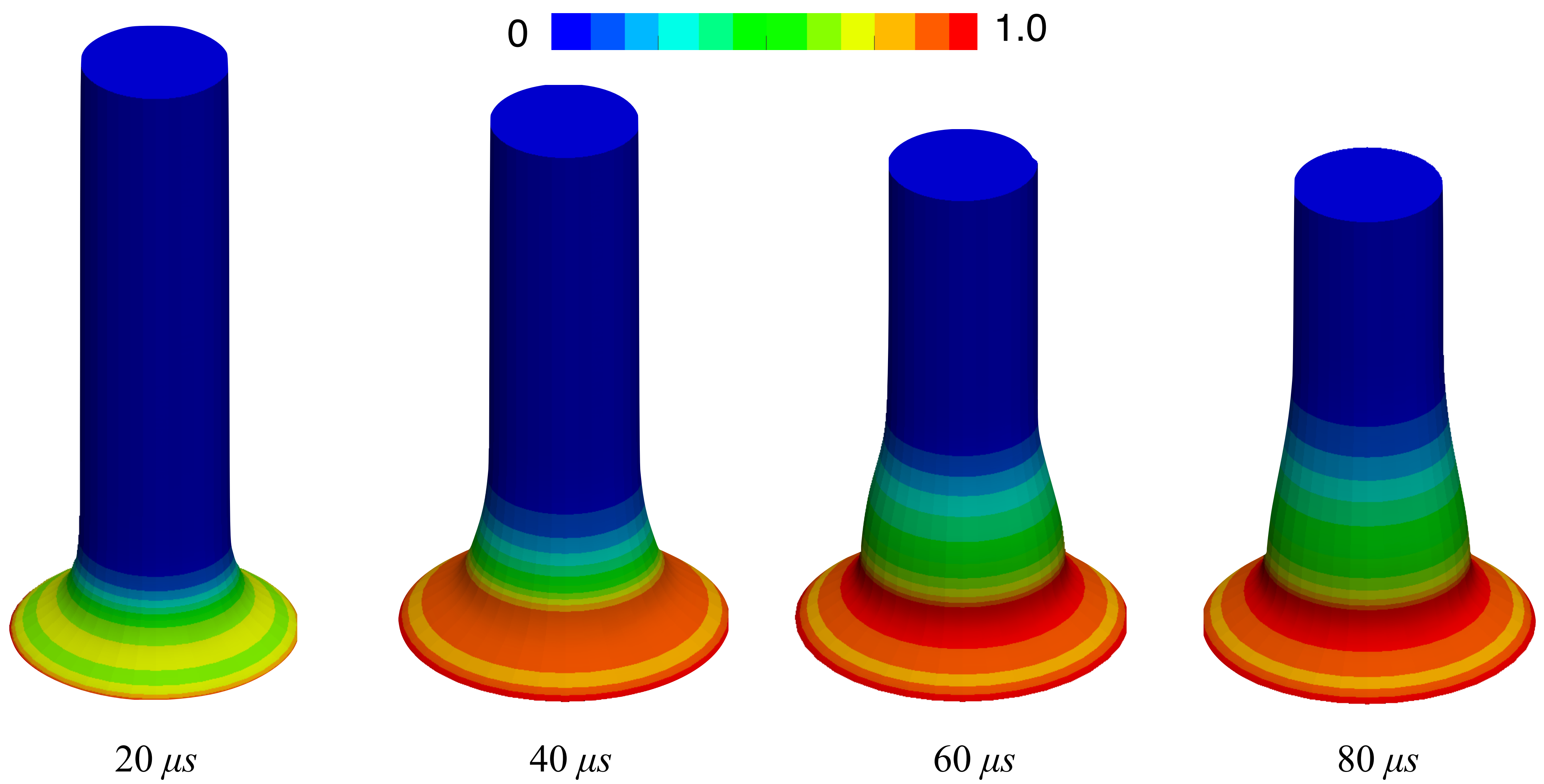

(a) Deformed geometry predicted by the current method

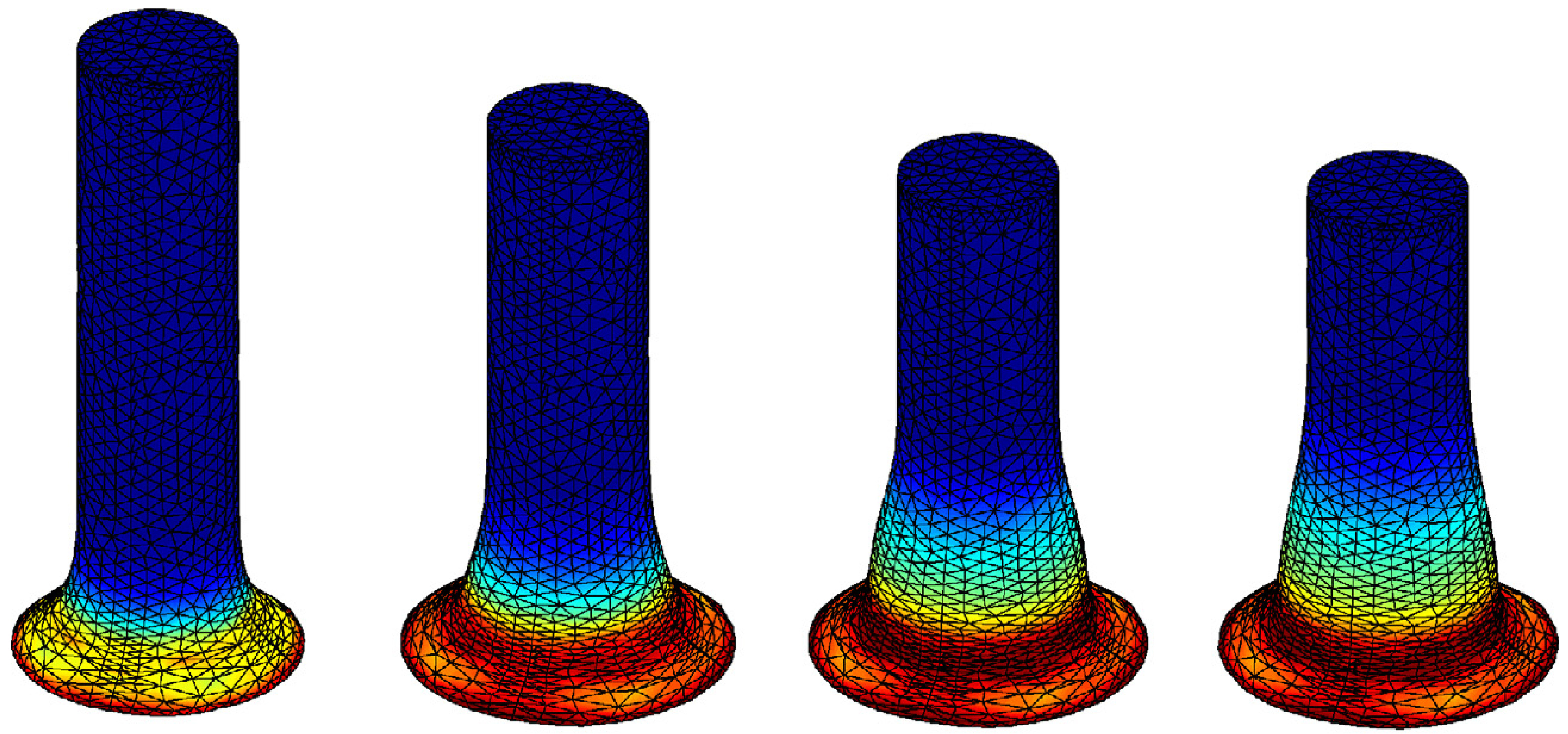

(b) Deformed geometry predicted by Aguirre et al. [54]

Summary
&
Conclusions

Summary & Conclusions

OpenFOAM solvers have been developed with the significant capabilities for solid mechanics analyses, where strict benchmarking against industry standard commercial software has been performed.

For **linear** problems:

- Fully implicit block-coupled procedure for linear elasticity
- Impressive efficiency compared with standard FE approaches
- Equivalent accuracy to standard linear FE approaches

For **nonlinear** problems:

- A large strain elasto-plastic updated Lagrangian solver with frictional contact boundary conditions
- straight-forward implementation of complex nonlinear constitutive laws
- Efficient parallelisation

26th to 30th June 2016

11th OpenFOAM Workshop
Vila Flor Cultural Centre
Guimarães, Portugal

Performance of Lagrangian Finite Volume Approaches for Linear and Nonlinear Solid Mechanics Analyses

Philip Cardiff

Željko Tukovic
Michael Clancy
Hrvoje Jasak
Peter De Jaeger
Alojz Ivanković

School of Mechanical and Materials Engineering
University College Dublin

UCD DUBLIN

BEKAERT better together

IComp Irish Centre for Composites Research

References

[1] P. Cardiff, Z. Tukovic´, H. Jasak, and A. Ivankovic´, “A block-coupled finite volume methodology for linear elasticity and unstructured meshes,” Computers and structures, 2016, under review.

[2] P. Cardiff, Z. Tukovic´, P. D. Jaeger, and A. Ivankovic´, “A Lagrangian cell-centred finite volume method for metal forming simulation,” International journal for numerical methods in engineering, 2016, under review.

[3] P. Cardiff, A. Karac and A. Ivanković, “A large strain finite volume method for orthotropic bodies with general material directions”, Computer Methods in Applied Mechanics and Engineering, 268, 318-335, 2014.

[4] P. Cardiff, A. Karać, and A. Ivanković, “Development of a Finite Volume contact solver based on the penalty method”, Computational Materials Science, 03, 64:283–284, 2014.

[5] Ž. Tuković, A. Ivanković, and A. Karač, “Finite−Volume Stress Analysis in Multi−Material Linear Elastic Body”, International journal for numerical methods in engineering, vol. 93, no. 4, pp. 400–419, 2013.

[6] Ž. Tuković, H. Jasak, Updated Lagrangian finite volume solver for large deformation dynamic response of elastic body, Transactions of FAMENA 31(1):55, 2007.

[7] T. Tang, O. Hededal, P. Cardiff, On finite volume method implementation of poro-elasto-plasticity soil model, International journal for numerical and analytical methods in geomechanics, 2015, DOI: 10.1002/nag.2361.